Laboratory experiment on jets

and simulations

Martín Huarte-Espinosa
<martinhe@pas.rochester.edu>
Department of Physics
and Astronomy
University of Rochester

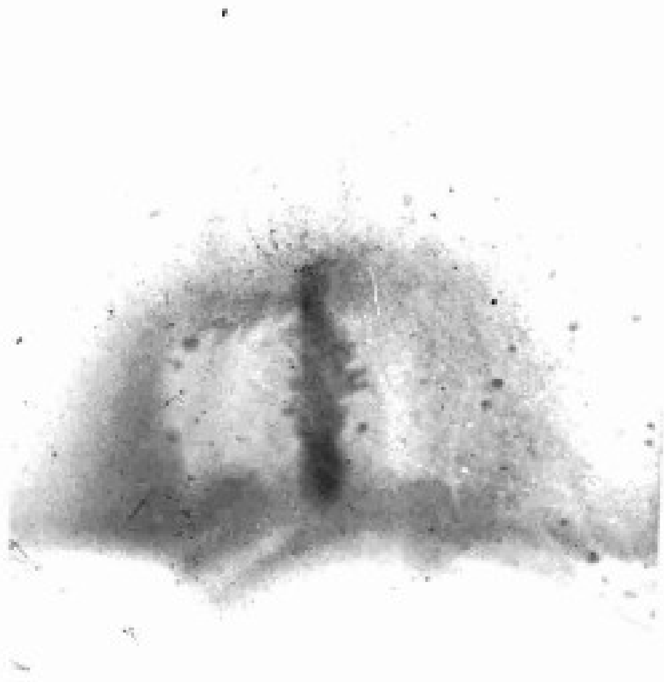

In collaboration with
Adam Frank & Eric Blackman
(University of Rochester)
Sergey Lebedev et al.
(Imperial College London)

MFU III, Zakopane, PL, 22/08/11

Motivation

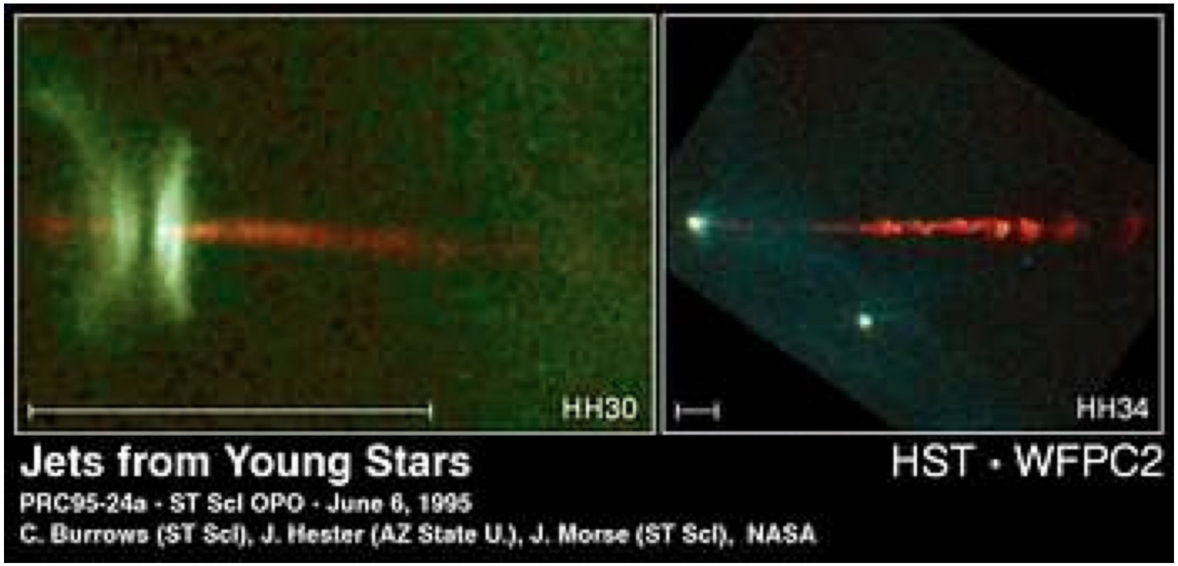

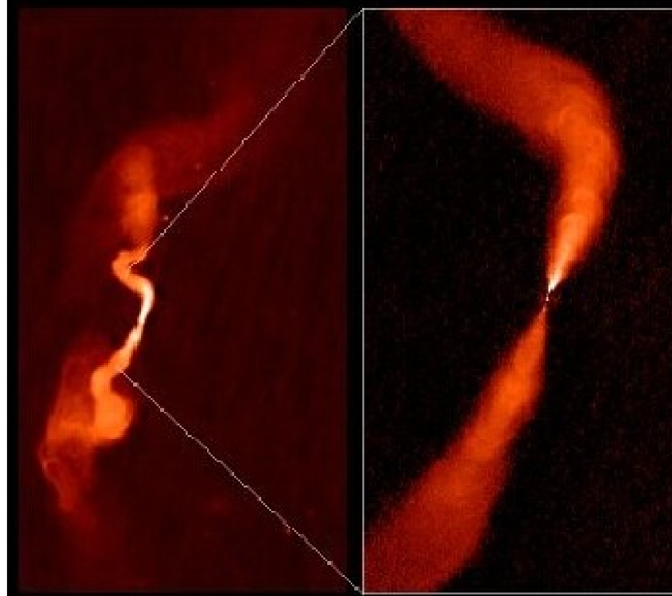
FR Class I source: radio galaxy 3C31


FR Class II source: quasar 3C175

From the AGN Atlas of Leahy, Bridle & Strom

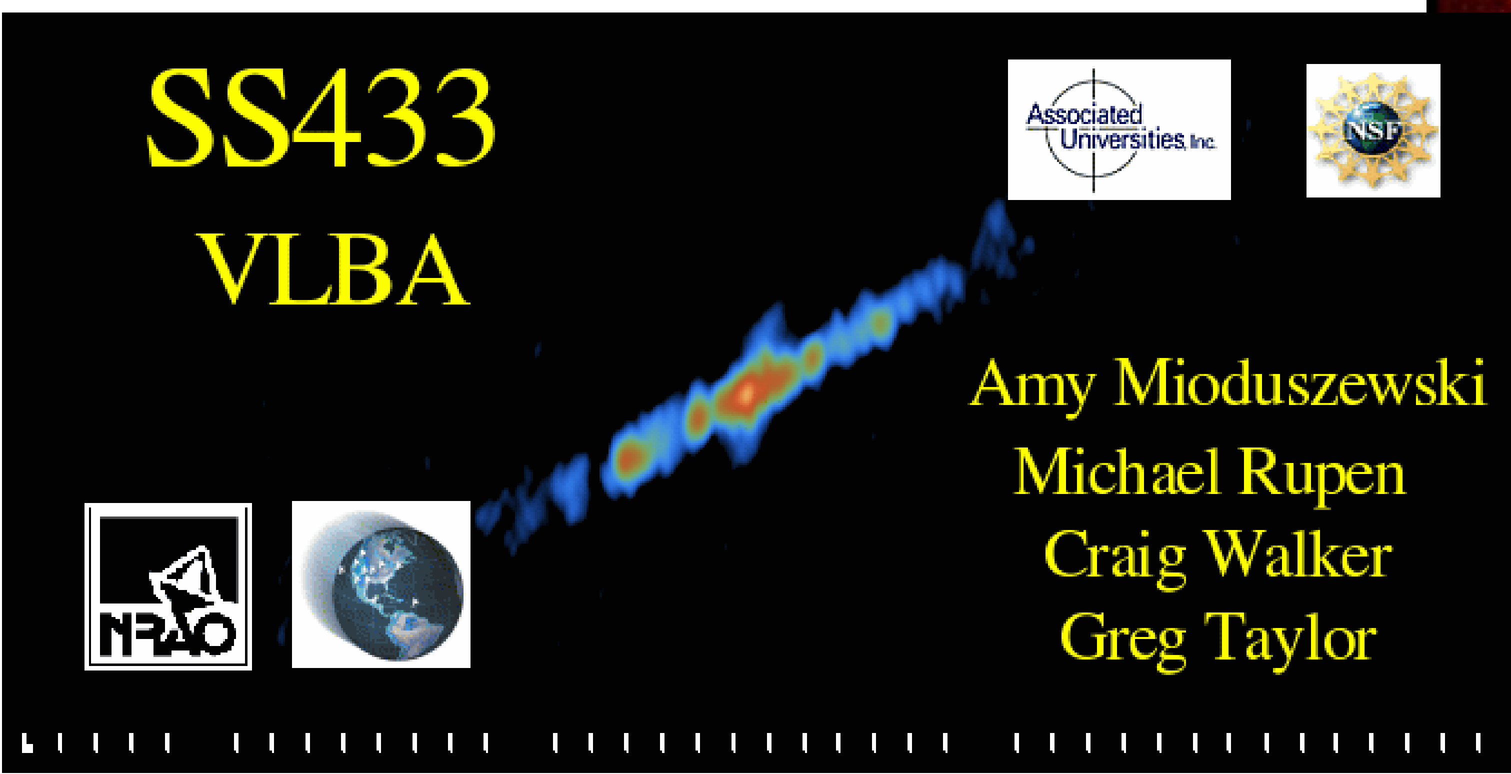

--- Poster ---

Interaction of FR II radio jets with a magnetised intra-cluster medium

Huarte-Espinosa, Krause & Alexander 2011c

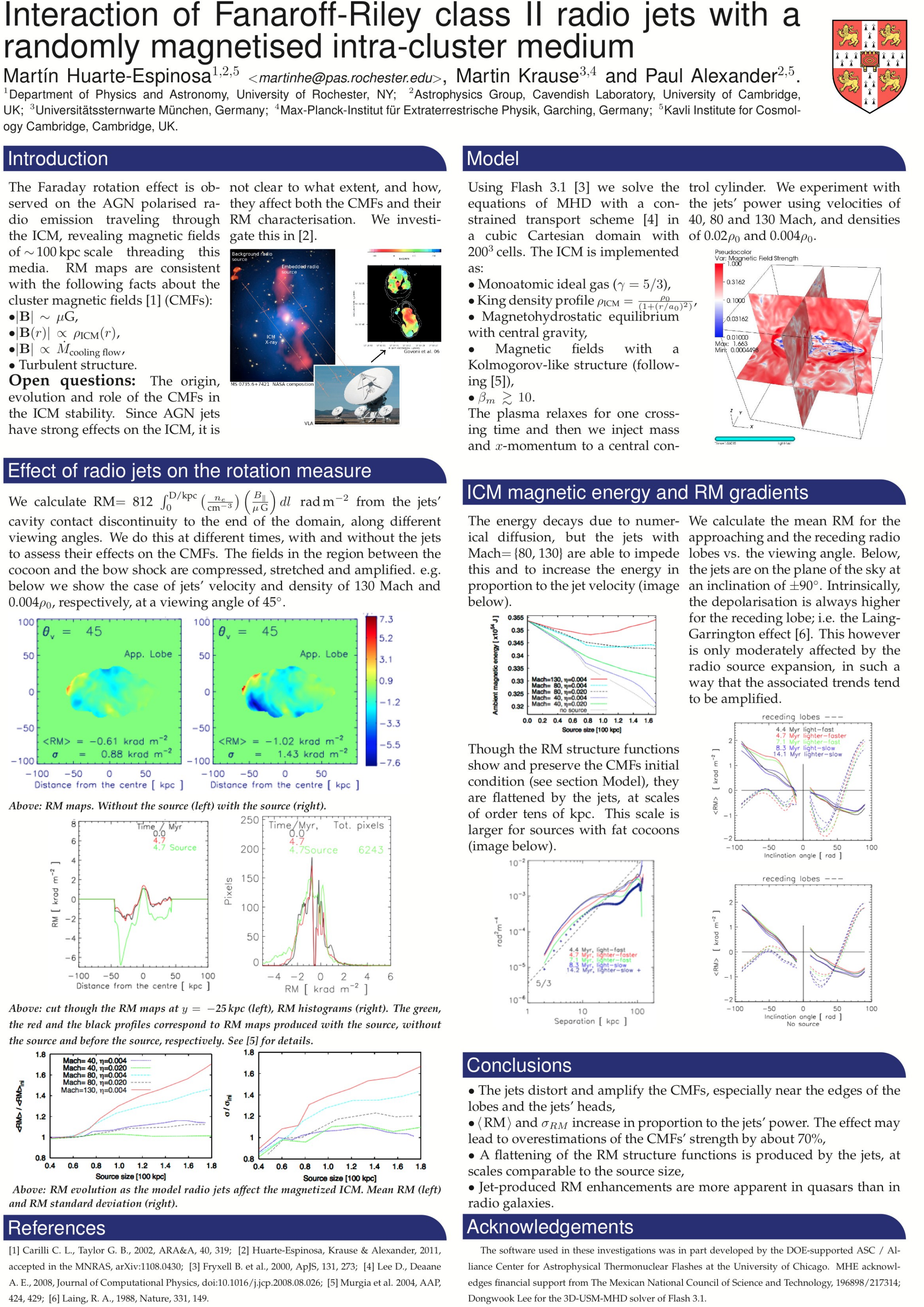

Interaction of Fanaroff-Riley class II radio jets with a randomly magnetised intra-cluster medium

Martín Huarte-Espinosa[1,2,5] <martinhe@pas.rochester.edu>, Martin Krause[3,4] and Paul Alexander[2,5].

[1]Department of Physics and Astronomy, University of Rochester, NY; [2]Astrophysics Group, Cavendish Laboratory, University of Cambridge, UK; [3]Universitätssternwarte München, Germany; [4]Max-Planck-Institut für Extraterrestrische Physik, Garching, Germany; [5]Kavli Institute for Cosmology Cambridge, Cambridge, UK.

Introduction

The Faraday rotation effect is observed on the AGN polarised radio emission traveling through the ICM, revealing magnetic fields of ~ 100 kpc scale threading this media. RM maps are consistent with the following facts about the cluster magnetic fields [1] (CMFs):

- $|\mathbf{B}| \sim \mu$G,
- $|\mathbf{B}(r)| \propto \rho_{\rm ICM}(r)$,
- $|\mathbf{B}| \propto \dot{M}_{\rm cooling\ flow}$,
- Turbulent structure.

Open questions: The origin, evolution and role of the CMFs in the ICM stability. Since AGN jets have strong effects on the ICM, it is not clear to what extent, and how, they affect both the CMFs and their RM characterisation. We investigate this in [2].

Model

Using Flash 3.1 [3] we solve the equations of MHD with a constrained transport scheme [4] in a cubic Cartesian domain with 200^3 cells. The ICM is implemented as:

- Monoatomic ideal gas ($\gamma = 5/3$),
- King density profile $\rho_{\rm ICM} = \frac{\rho_0}{(1+(r/a_0)^2)}$,
- Magnetohydrostatic equilibrium with central gravity,
- Magnetic fields with a Kolmogorov-like structure (following [5]),
- $\beta_m \gtrsim 10$.

The plasma relaxes for one crossing time and then we inject mass and x-momentum to a central control cylinder. We experiment with the jets' power using velocities of 40, 80 and 130 Mach, and densities of $0.02\rho_0$ and $0.004\rho_0$.

Effect of radio jets on the rotation measure

We calculate RM$= 812 \int_0^{D/{\rm kpc}} \left(\frac{n_e}{\rm cm^{-3}}\right)\left(\frac{B_\parallel}{\mu{\rm G}}\right) dl$ rad m^{-2} from the jets' cavity contact discontinuity to the end of the domain, along different viewing angles. We do this at different times, with and without the jets to assess their effects on the CMFs. The fields in the region between the cocoon and the bow shock are compressed, stretched and amplified. e.g. below we show the case of jets' velocity and density of 130 Mach and $0.004\rho_0$, respectively, at a viewing angle of 45°.

Above: RM maps. Without the source (left) with the source (right).

Above: cut though the RM maps at $y = -25$ kpc (left), RM histograms (right). The green, the red and the black profiles correspond to RM maps produced with the source, without the source and before the source, respectively. See [5] for details.

Above: RM evolution as the model radio jets affect the magnetized ICM. Mean RM (left) and RM standard deviation (right).

ICM magnetic energy and RM gradients

The energy decays due to numerical diffusion, but the jets with Mach={80, 130} are able to impede this and to increase the energy in proportion to the jet velocity (image below).

Though the RM structure functions show and preserve the CMFs initial condition (see section Model), they are flattened by the jets, at scales of order tens of kpc. This scale is larger for sources with fat cocoons (image below).

We calculate the mean RM for the approaching and the receding radio lobes vs. the viewing angle. Below, the jets are on the plane of the sky at an inclination of ±90°. Intrinsically, the depolarisation is always higher for the receding lobe; i.e. the Laing-Garrington effect [6]. This however is only moderately affected by the radio source expansion, in such a way that the associated trends tend to be amplified.

Conclusions

- The jets distort and amplify the CMFs, especially near the edges of the lobes and the jets' heads,
- $\langle$RM$\rangle$ and σ_{RM} increase in proportion to the jets' power. The effect may lead to overestimations of the CMFs' strength by about 70%,
- A flattening of the RM structure functions is produced by the jets, at scales comparable to the source size,
- Jet-produced RM enhancements are more apparent in quasars than in radio galaxies.

References

[1] Carilli C. L., Taylor G. B., 2002, ARA&A, 40, 319; [2] Huarte-Espinosa, Krause & Alexander, 2011, accepted in the MNRAS, arXiv:1108.0430; [3] Fryxell B. et al., 2000, ApJS, 131, 273; [4] Lee D., Deaane A. E., 2008, Journal of Computational Physics, doi:10.1016/j.jcp.2008.08.026; [5] Murgia et al. 2004, AAP, 424, 429; [6] Laing, R. A., 1988, Nature, 331, 149.

Acknowledgements

The software used in these investigations was in part developed by the DOE-supported ASC / Alliance Center for Astrophysical Thermonuclear Flashes at the University of Chicago. MHE acknowledges financial support from The Mexican National Council of Science and Technology, 196898/217314; Dongwook Lee for the 3D-USM-MHD solver of Flash 3.1.

Outline

le about magnetic fields in astro jets,

oratory **Experiments** (3),

Setups,

Results,

ulations of magnetic towers,

Model and methods,

Results,

mary.

Jet launch

Ingredients:
-1 **compact object**
-some **accreted** plasma
-some **magnetic fields**

Preparation:
Stir (**rotation**) vigorously until a hot disk is formed and the magnetic fields are helical & strong
Enjoy!

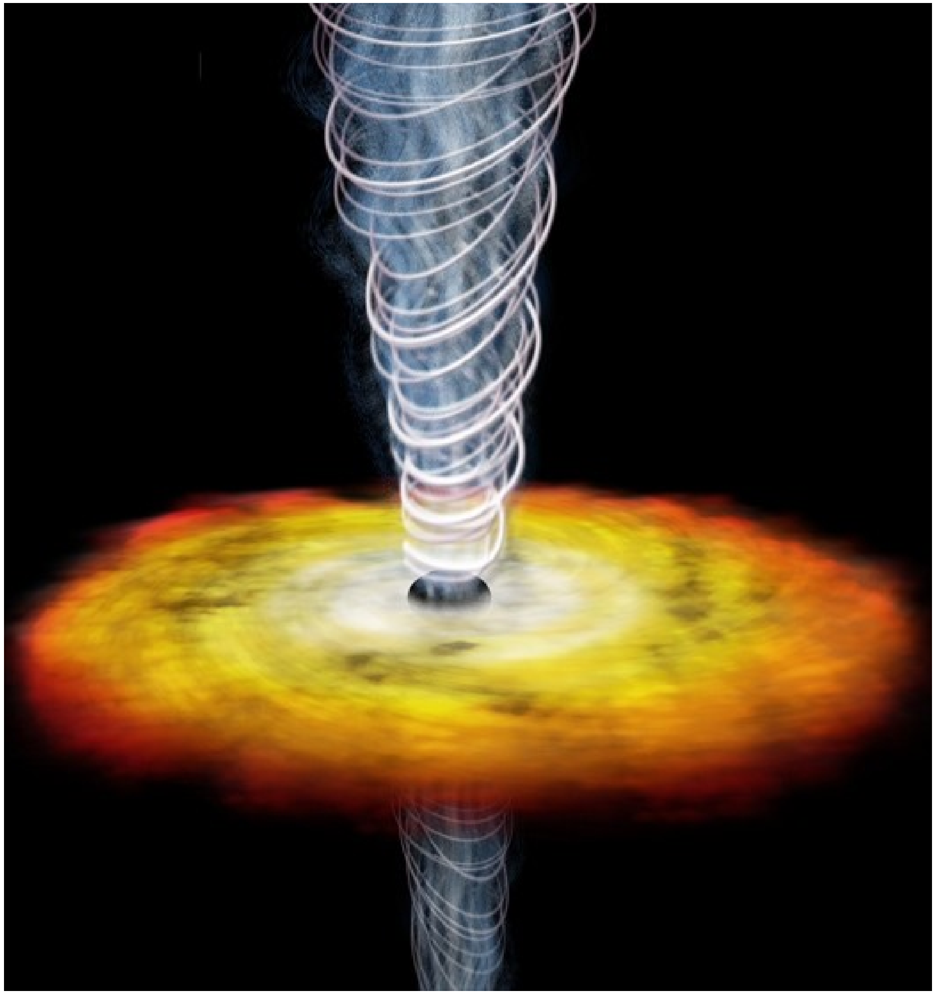

Magnetocentrifugal jets (Blandford & Payne 1982; Ouyed & Pudritz 1997; Ustyugova et al. 1999; Blackman et al. 2001)

→ *magnetic fields only dominate out to the Alfvén radius*

Poynting flux dominated jets (**PFD**; Lynden-Bell 1996; Ustyugova et al. ‘00; Li et al. ‘01; Lovelace et al. ‘02; Nakamura & Meier ‘04)

→ *magnetic fields dominate the jet structure*

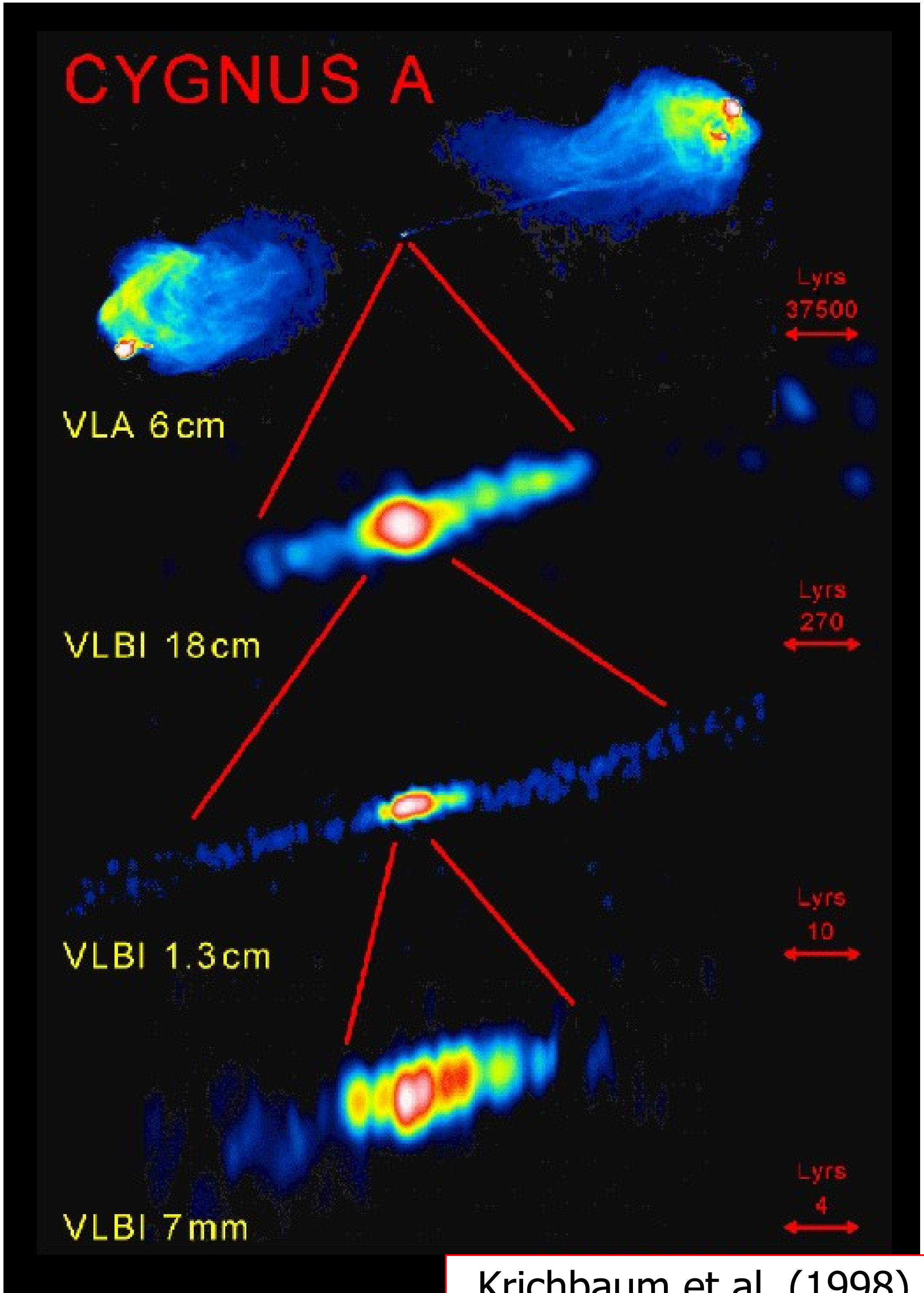

Krichbaum et al. (1998)

$|\mathbf{B}|_{weak}$

$|\mathbf{B}|_{weak}$

$|\mathbf{B}|_{?}$

$|\mathbf{B}|_{strong}$

Laboratory experiments

PFD jets, or magnetic towers, produced in a MAGPIE generator at Imperial College London

1. Radial wire array, Lebedev et al. ‘05,

   - Followed with MHD simulations by Ciardi et al. ‘07,

2. Radial wire array + axial magnetic field, Suzuki-Vidal et al. ‘10,

3. Thin conducting foil, Suzuki-Vidal et al. ‘10; Lebedev et al. ‘10.

1. Radial wire array (Lebedev et al. ’05)

1MA pulse current flows radially through 16 x 13μm tungsten metallic wires a central electrode. ~1 MG toroidal magnetic field produced below the wires.

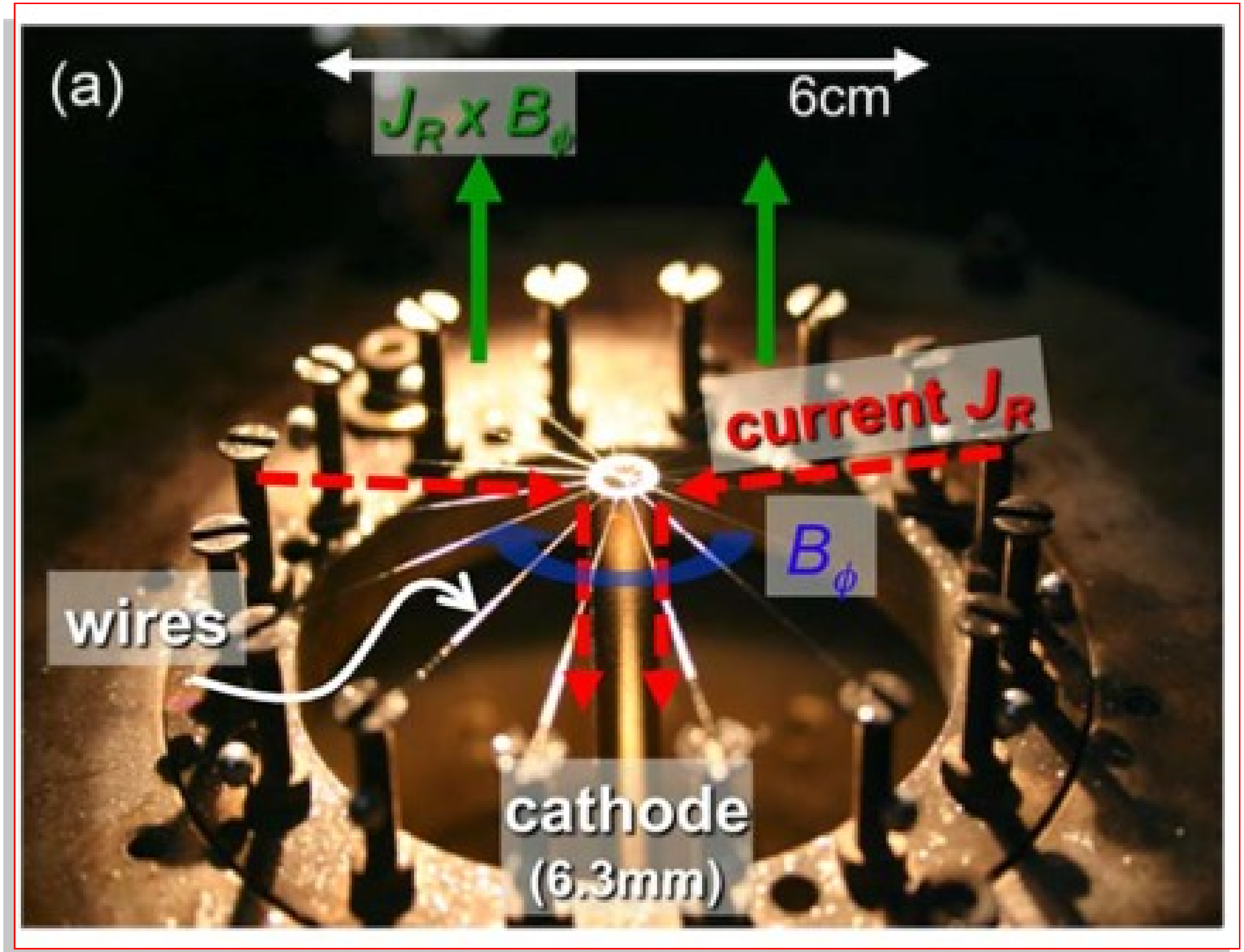

Evolution with XUV

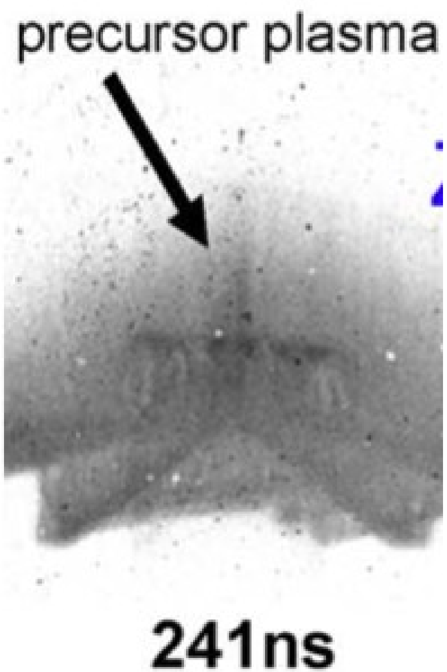

1.5cm

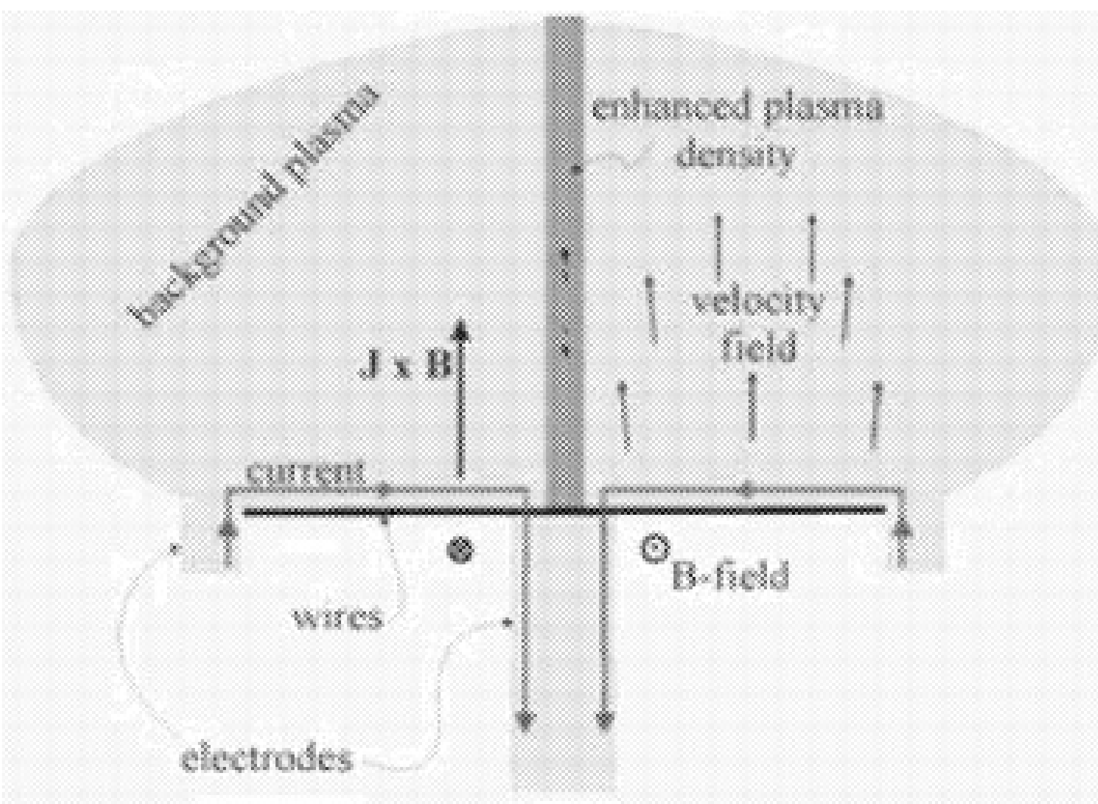

wire ablation + JxB force produce background plasma

resistive diffusion keeps current close to wires

Lebedev et al. 2005
Suzuki-Vidal et al. 2010

Evolution with XUV

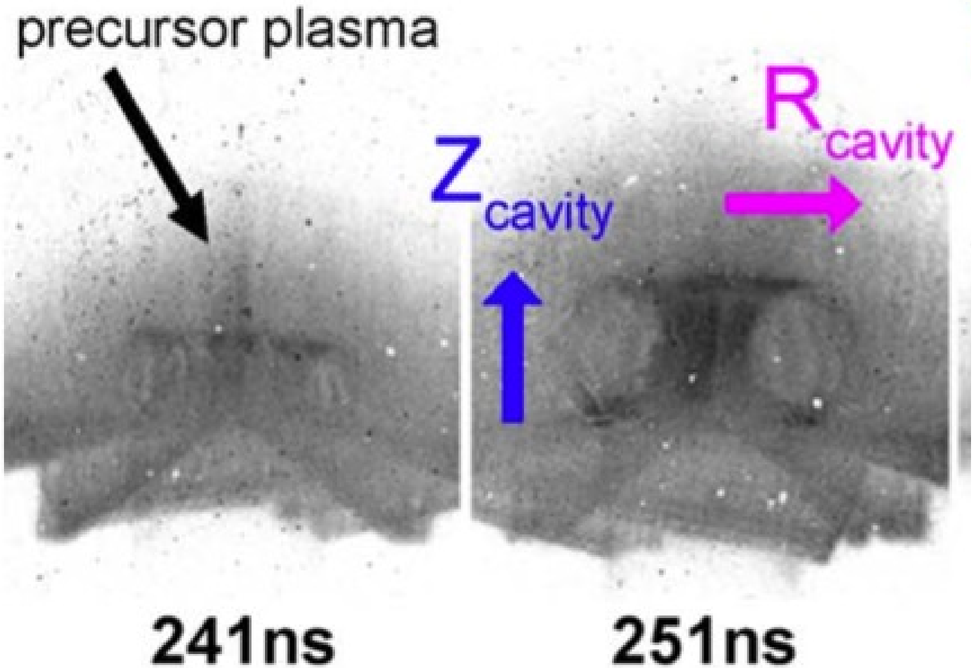

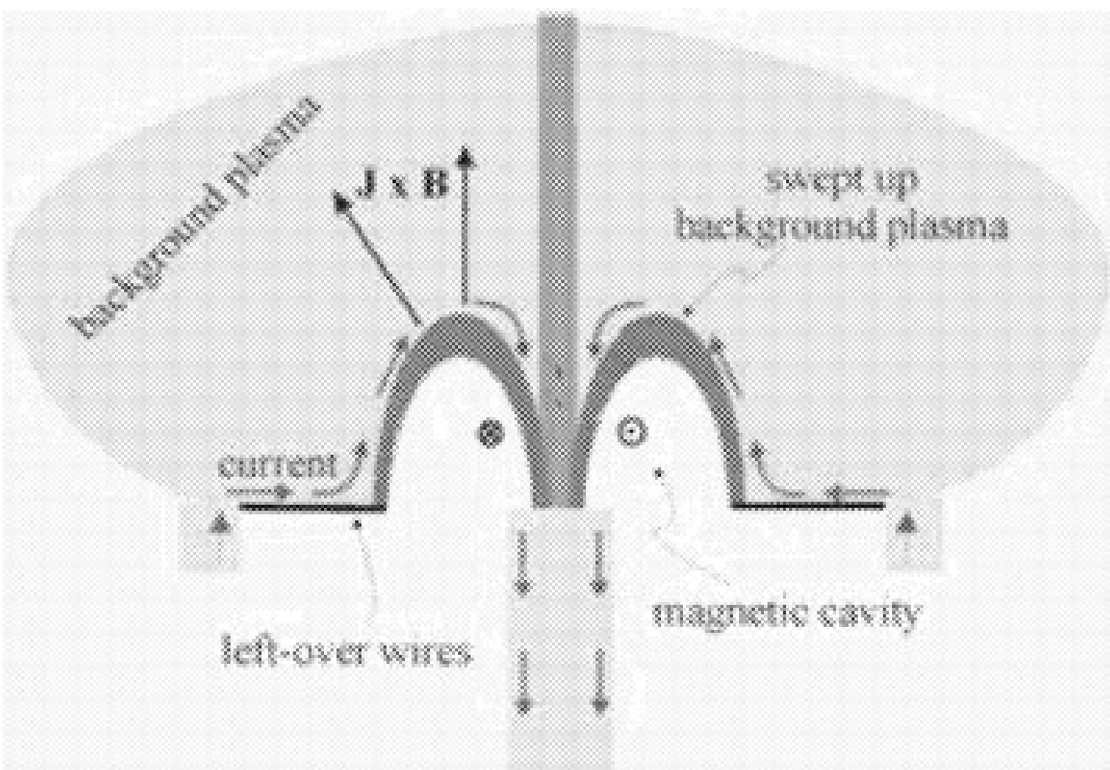

Full wire ablation near the central electrode forms a magnetic cavity.

Lebedev et al. 2005
Suzuki-Vidal et al. 2010

Evolution with XUV

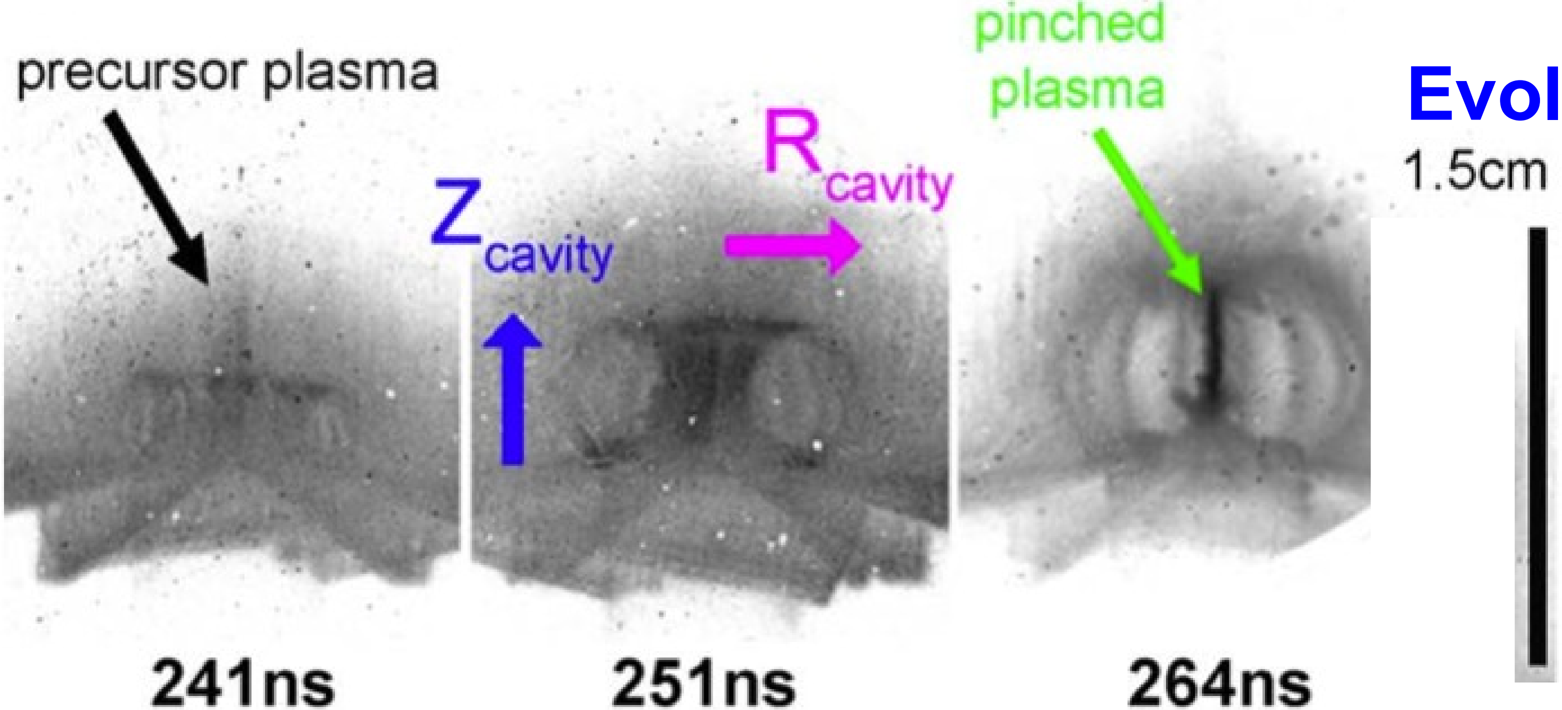

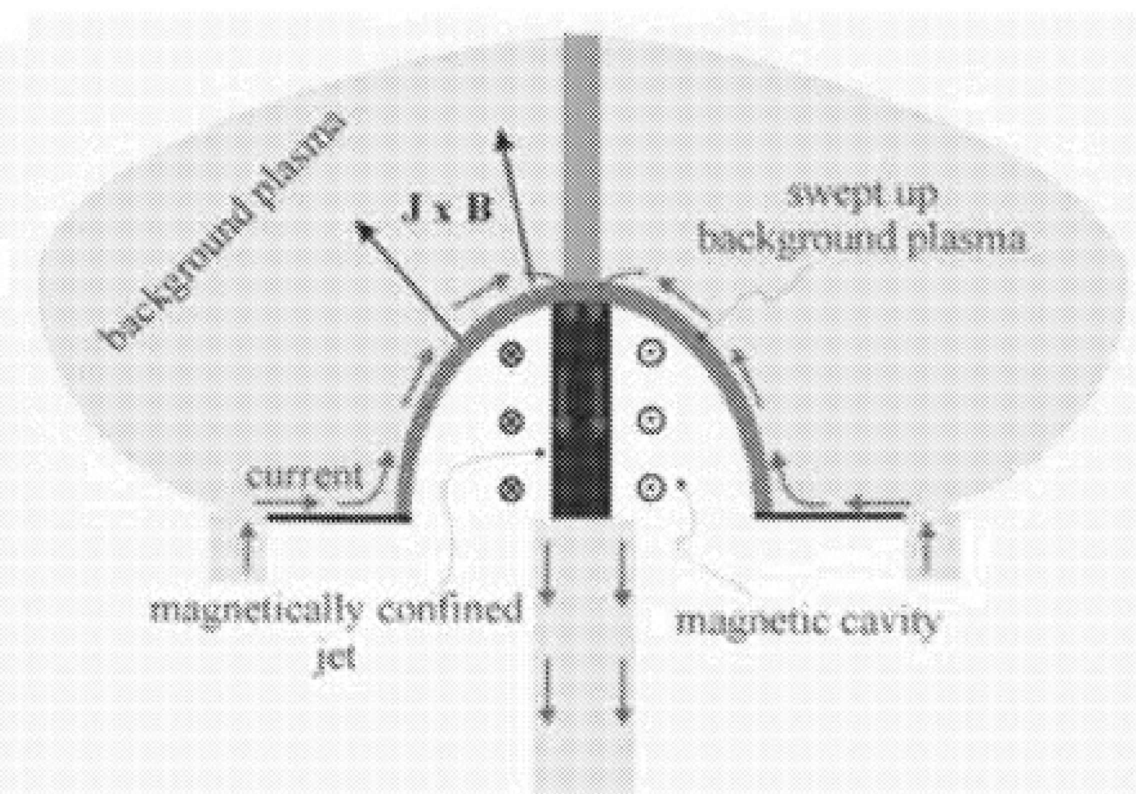

Expanding magnetic tower jet driven upwards by toroidal magnetic field pressure

Lebedev et al. 2005
Suzuki-Vidal et al. 2010

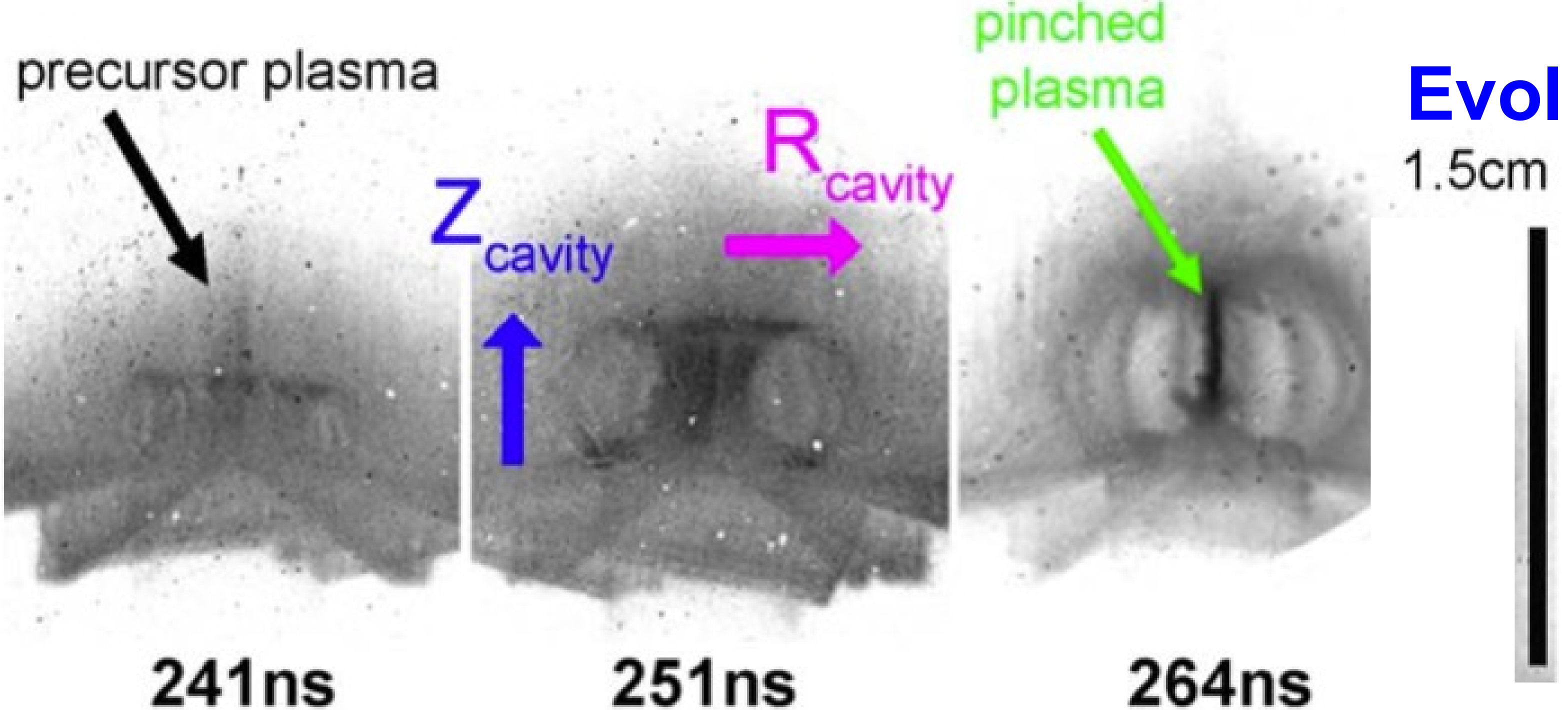

Evolution with XUV

Jet *Collimation* by hoop stress

Magnetic bubble *Collimation* by ambient medium

Consistent with Lynden-Bell ‘96, ‘03

Once the jet forms

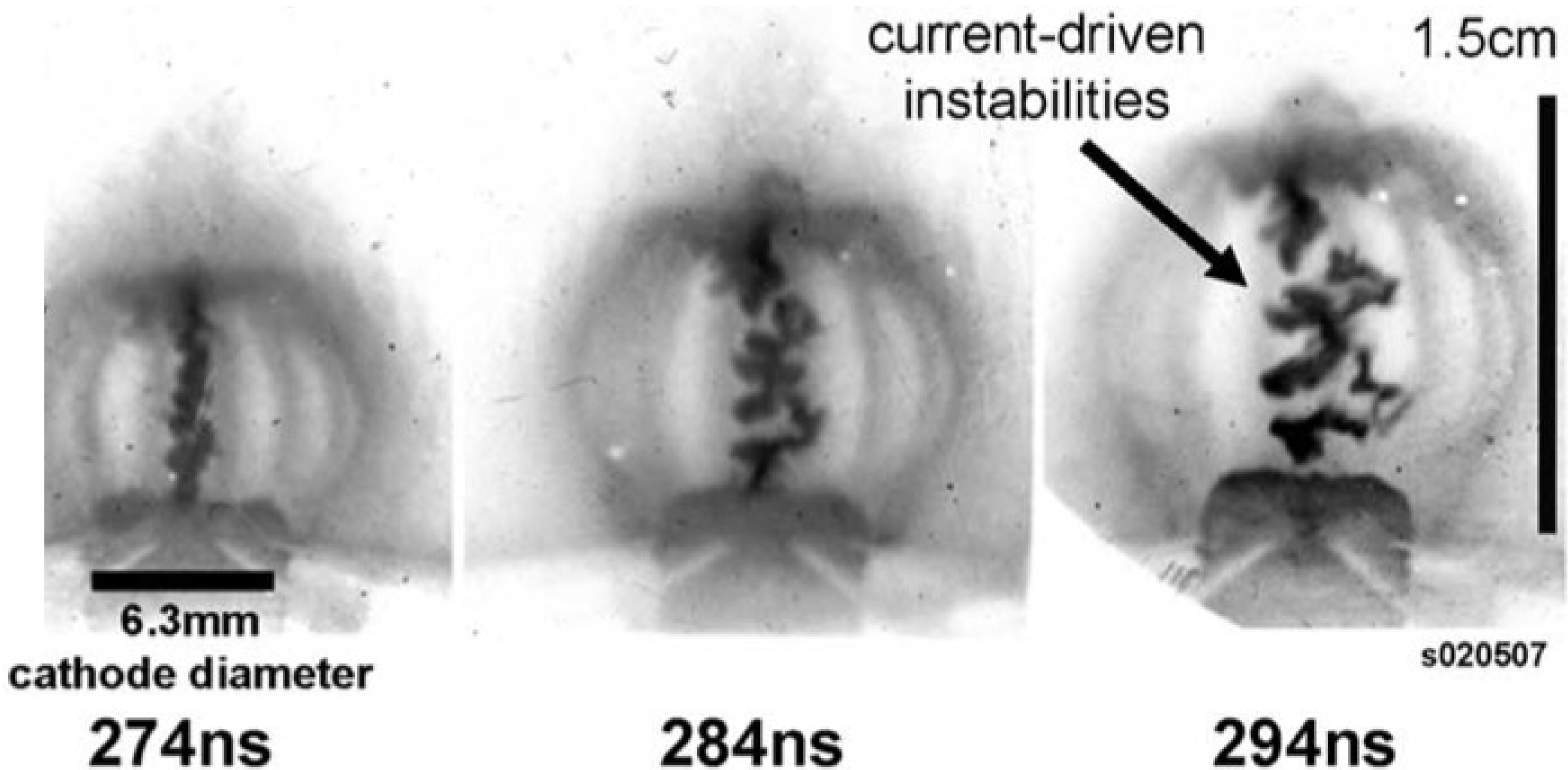

Lebedev et al. 2005
Suzuki-Vidal et al.
2010

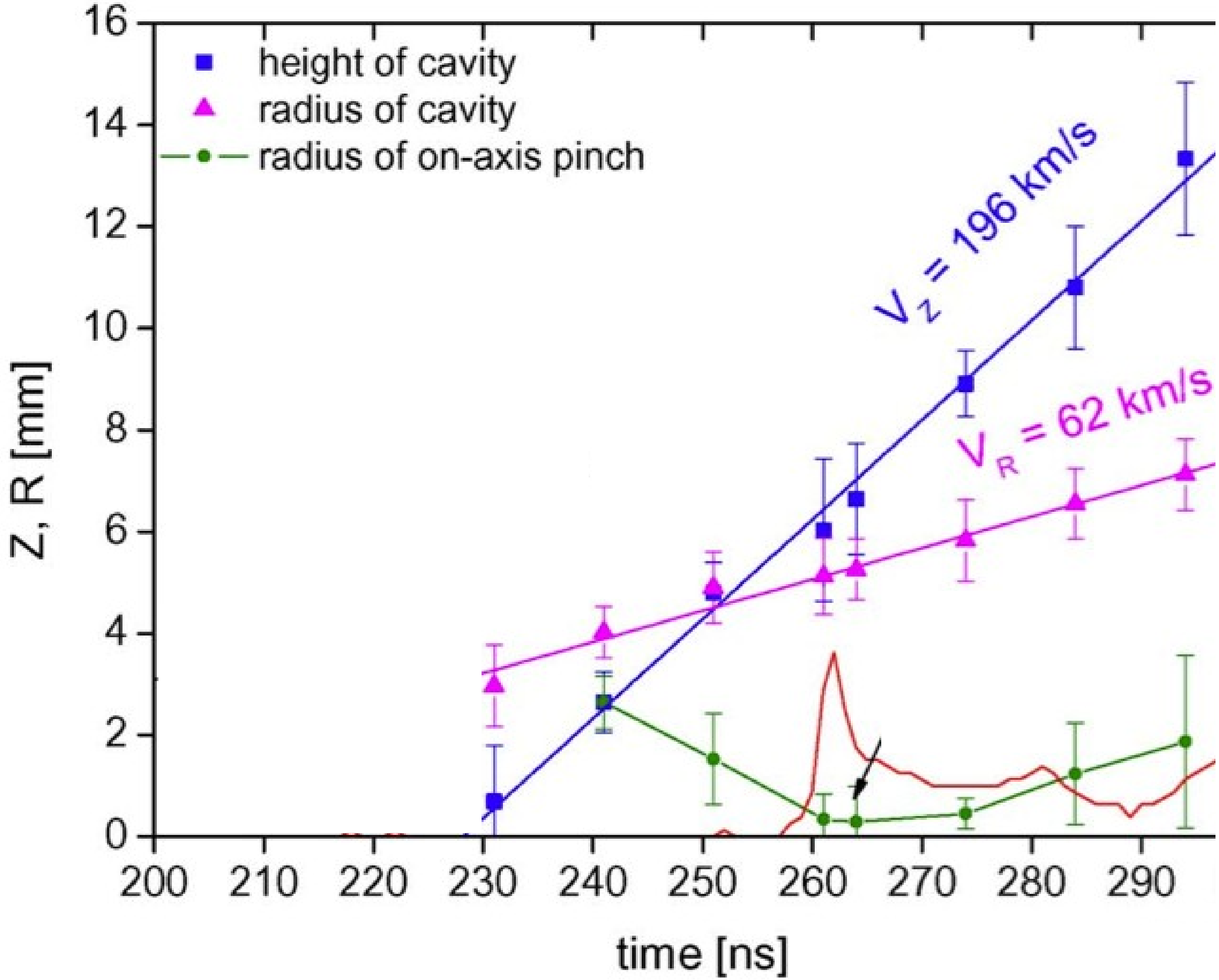

(Suzuki-Vidal et al. 2010)

Laser shadow images; electron density gradients (Lebedev et al. 2005).

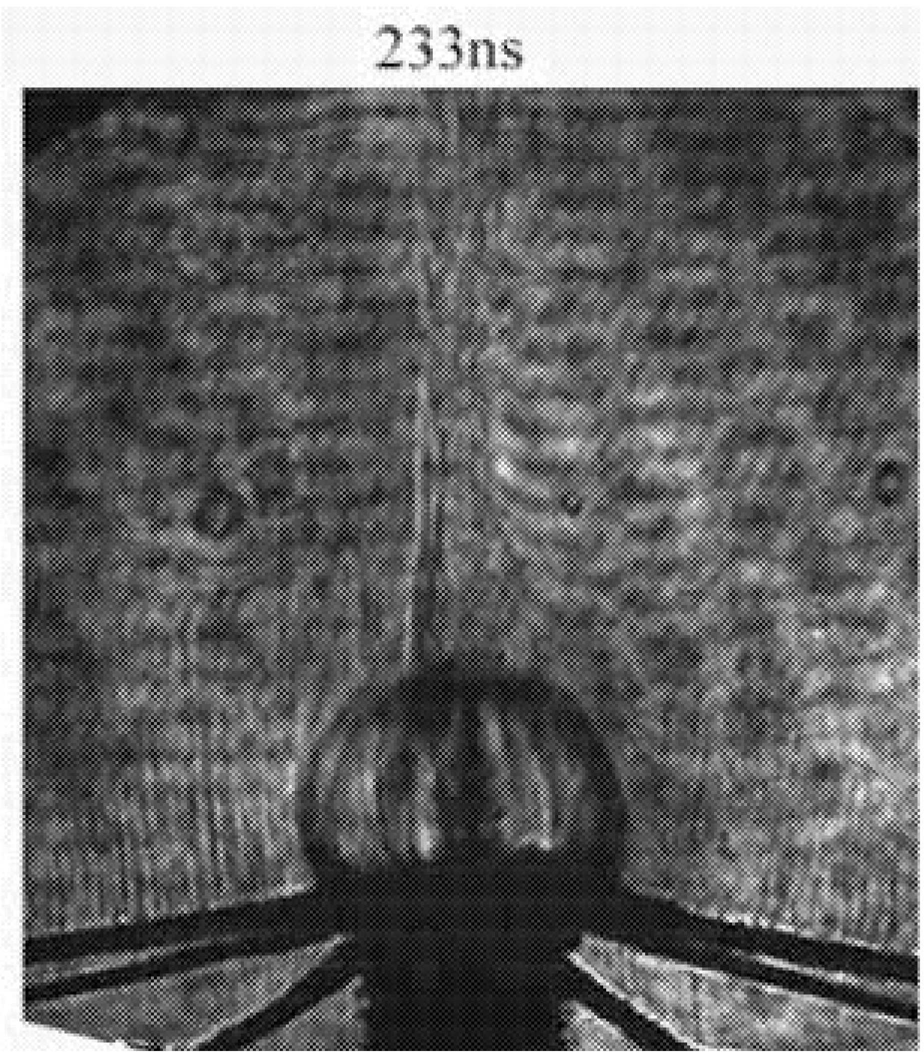

current

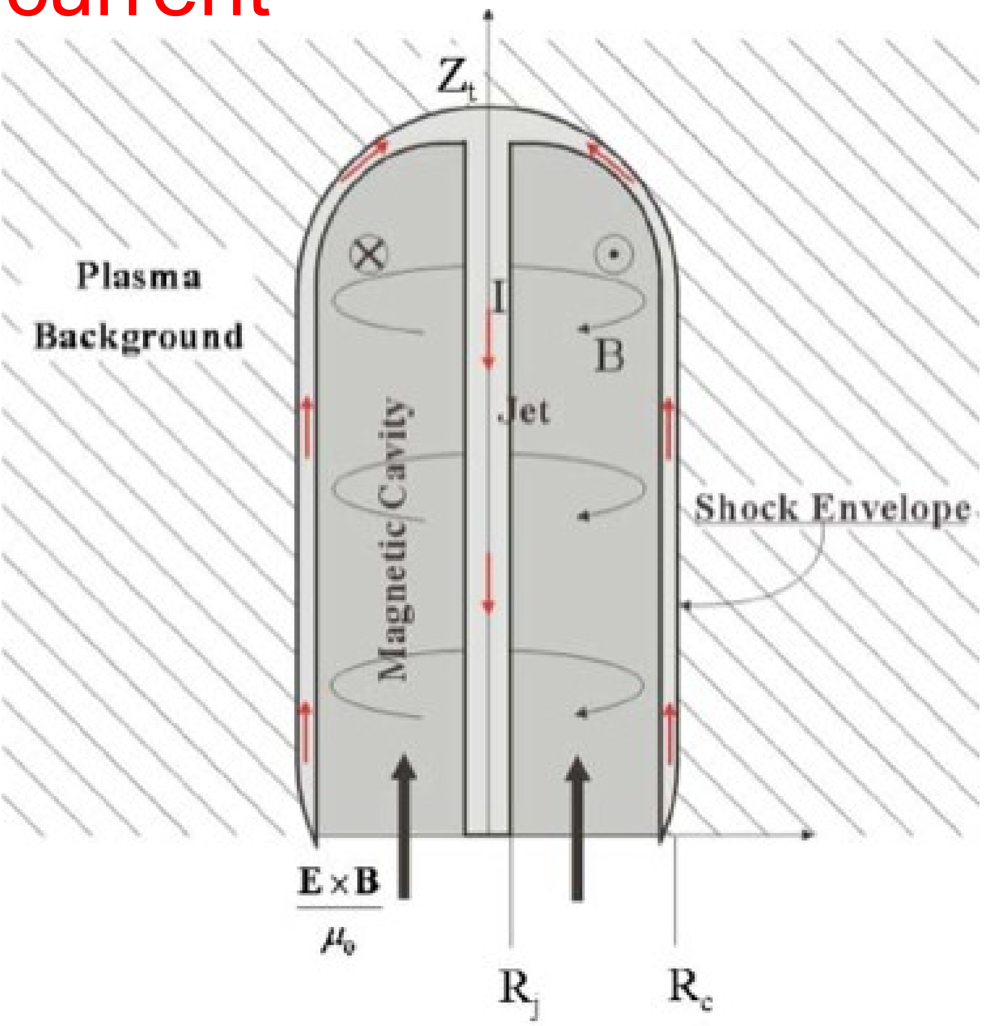

Simulations (Ciardi et al. 2007)

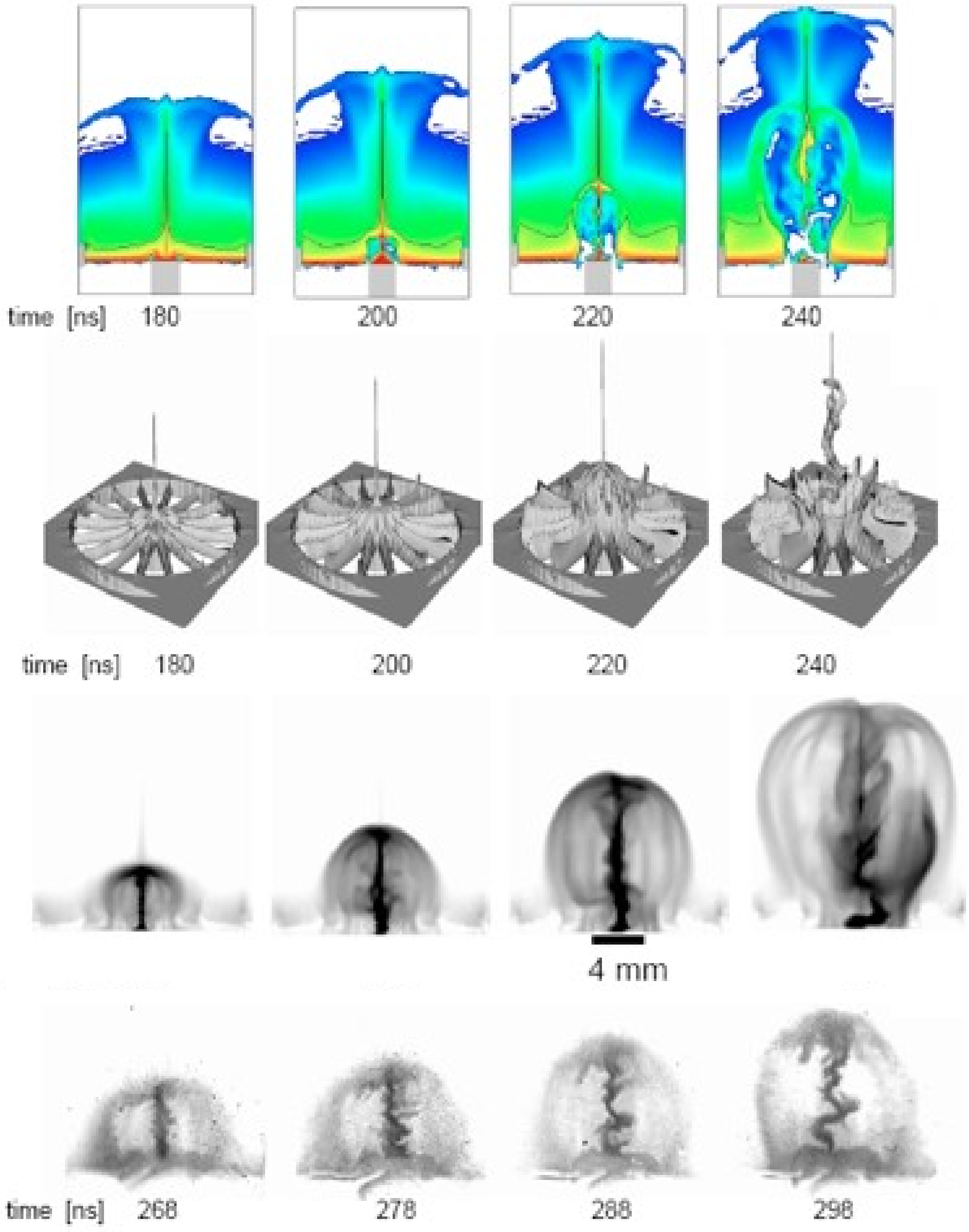

Density slices

Iso-density surfaces

Synthetic emission

XUV emission from **experiment** (again)

Model magnetic tower (Ciardi et al. 2007)

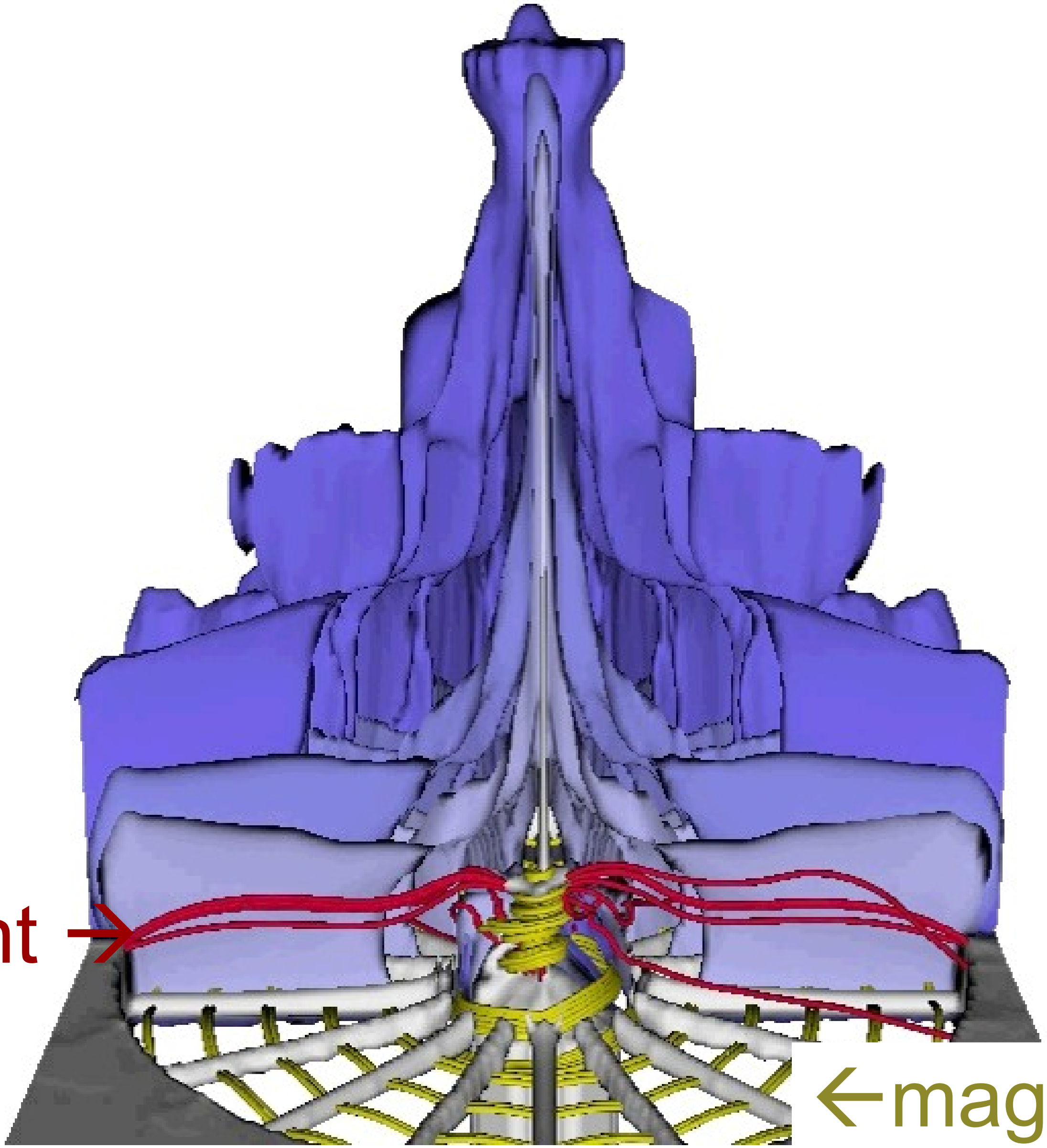

2. Radial wire array (again) + B_{axial}

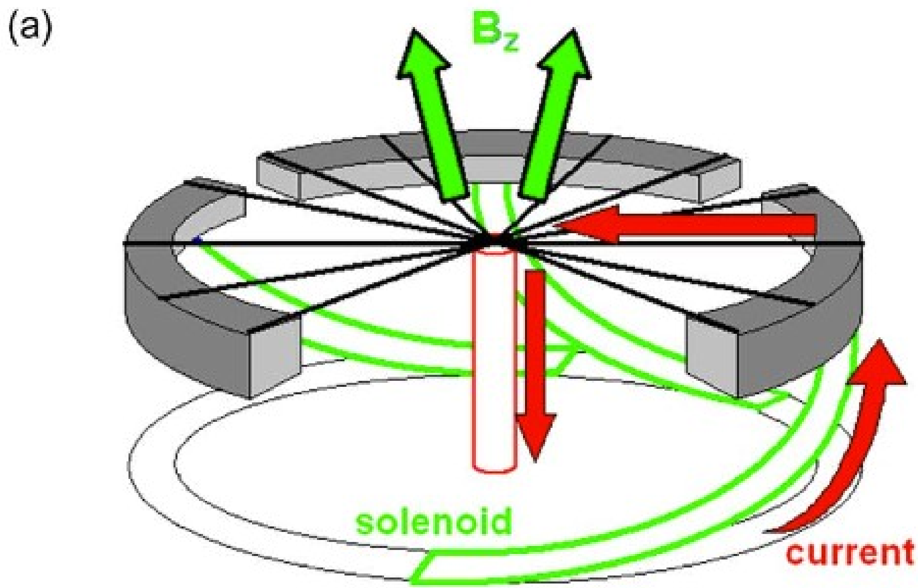

outer solenoid

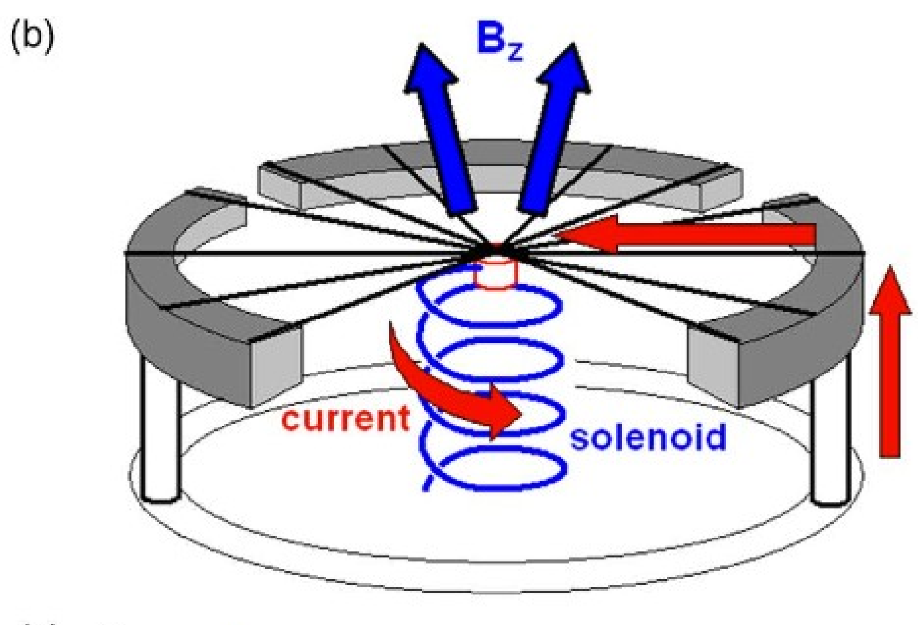

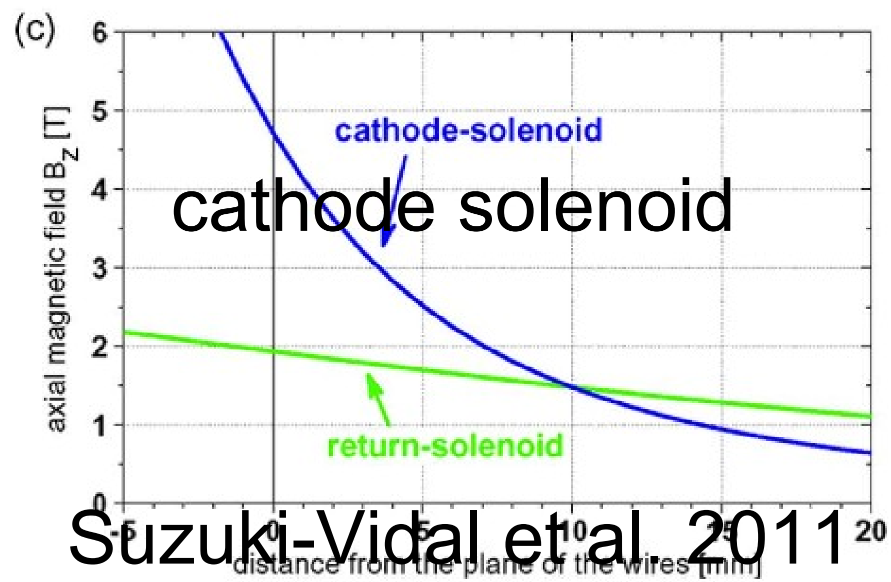

cathode solenoid

Suzuki-Vidal et al. 2011

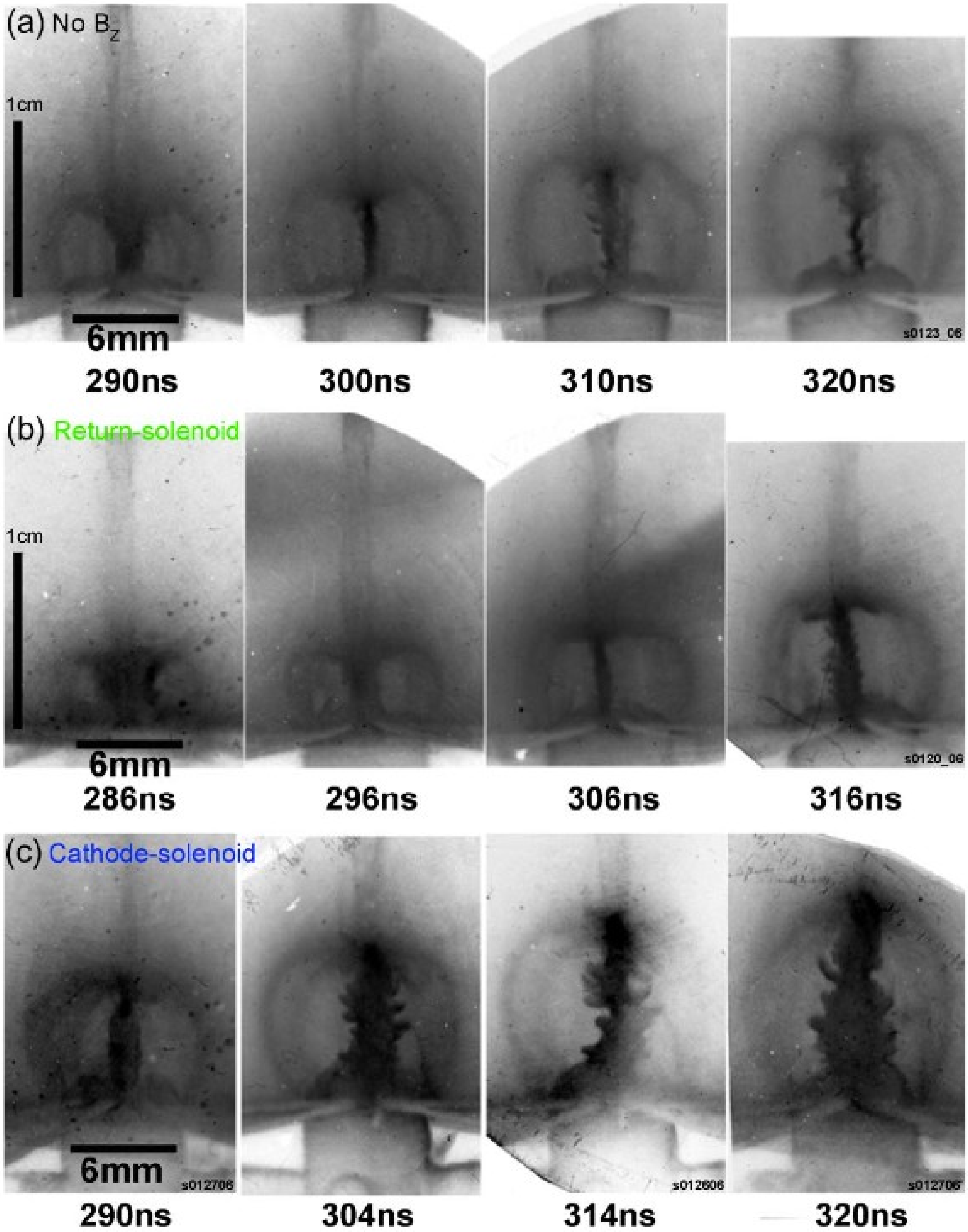

B_z affects axial compression

B_z α R_{column}

More stable

Suzuki-Vidal et al. '10

3. Thin conducting foil (Suzuki-Vidal et al. ‘10)

1MA, 250ns radial current pulse : ~1 MG toroidal magnetic

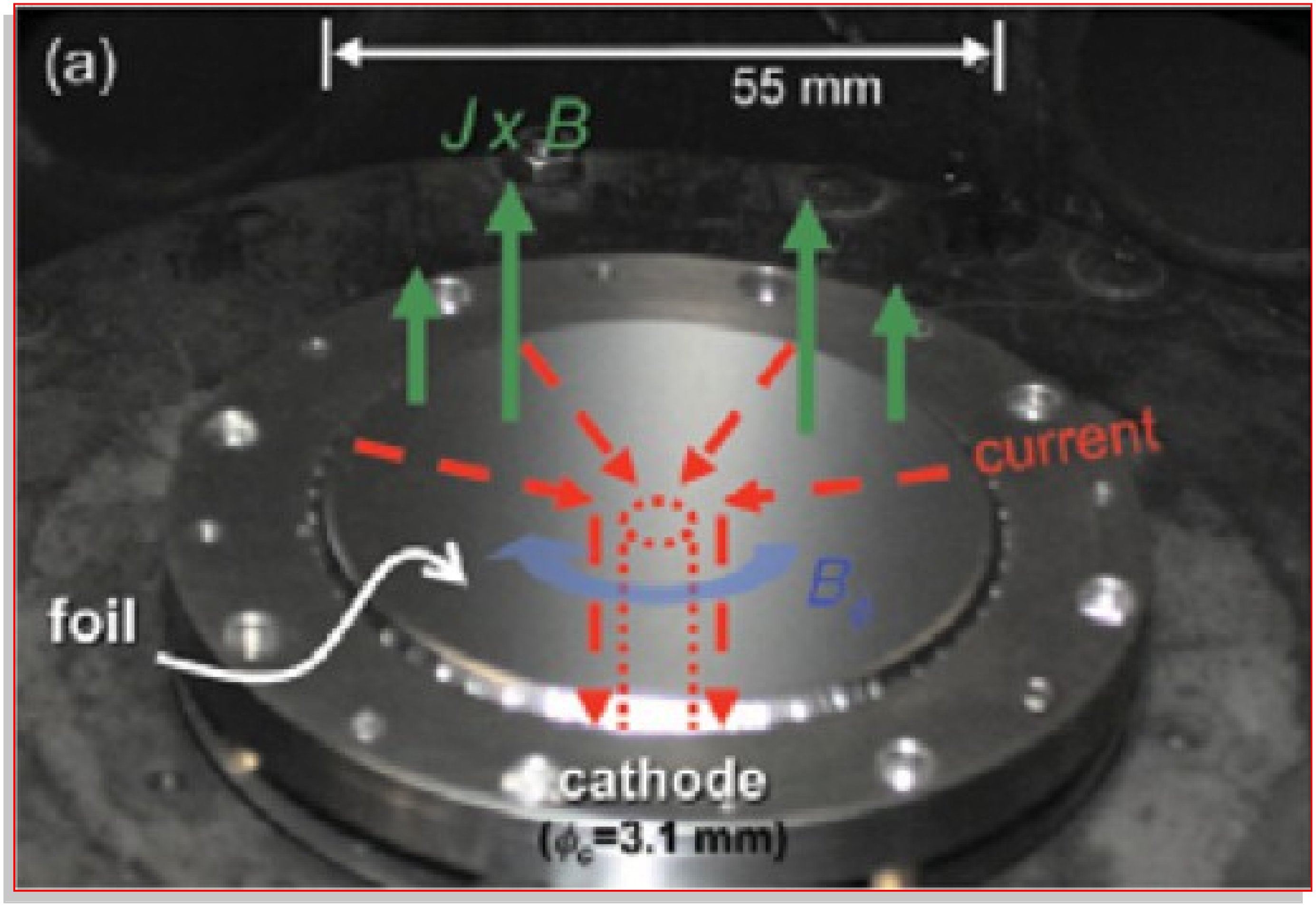

Lebedev et al. 2011

Foil

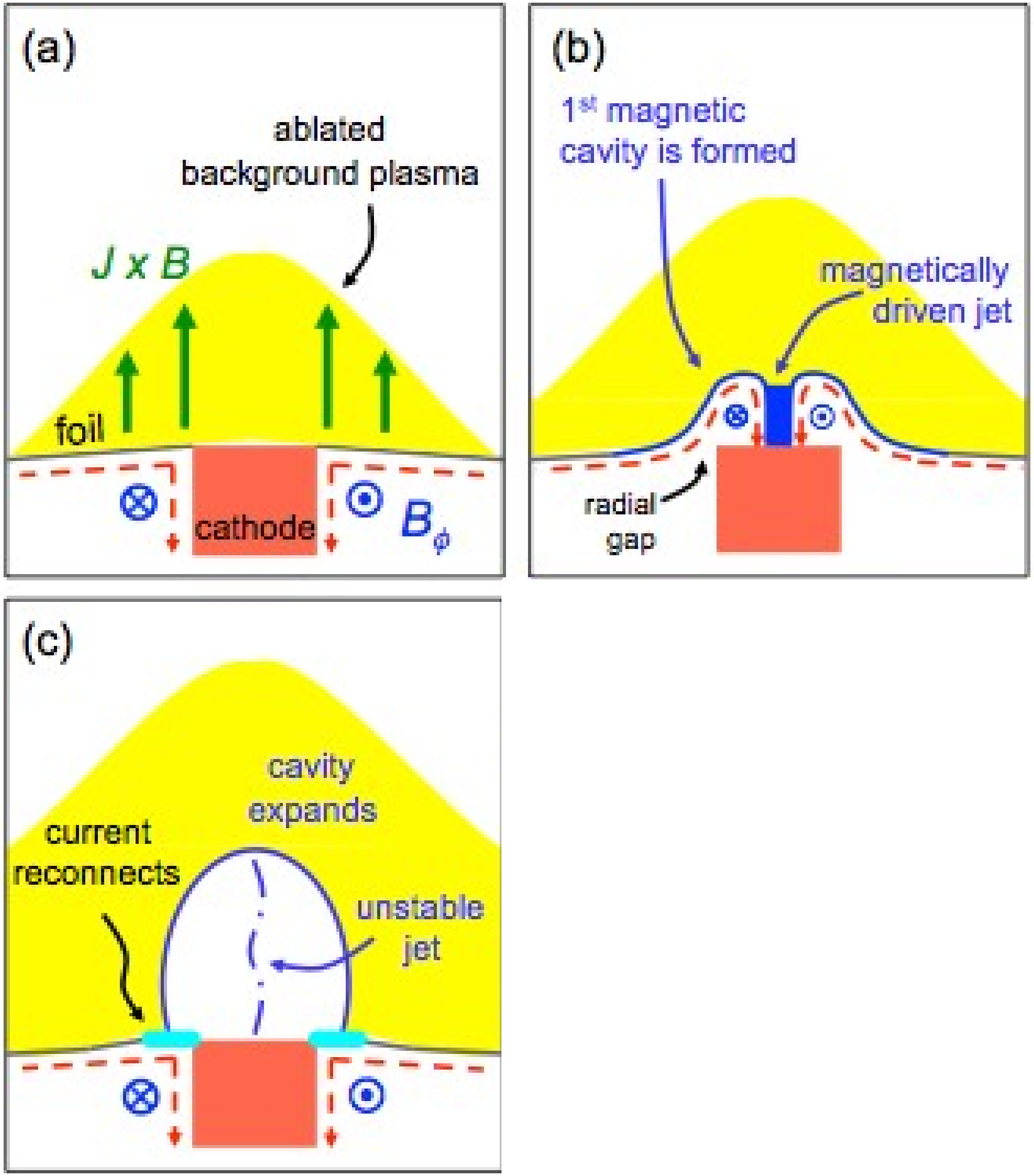

(a)
ablated
background plasma
J x B
foil
cathode
B_ϕ
(b)
1st magnetic
cavity is formed
magnetically
driven jet
radial
gap
(c)
cavity
expands
current
reconnects
unstable
jet

again

Foil

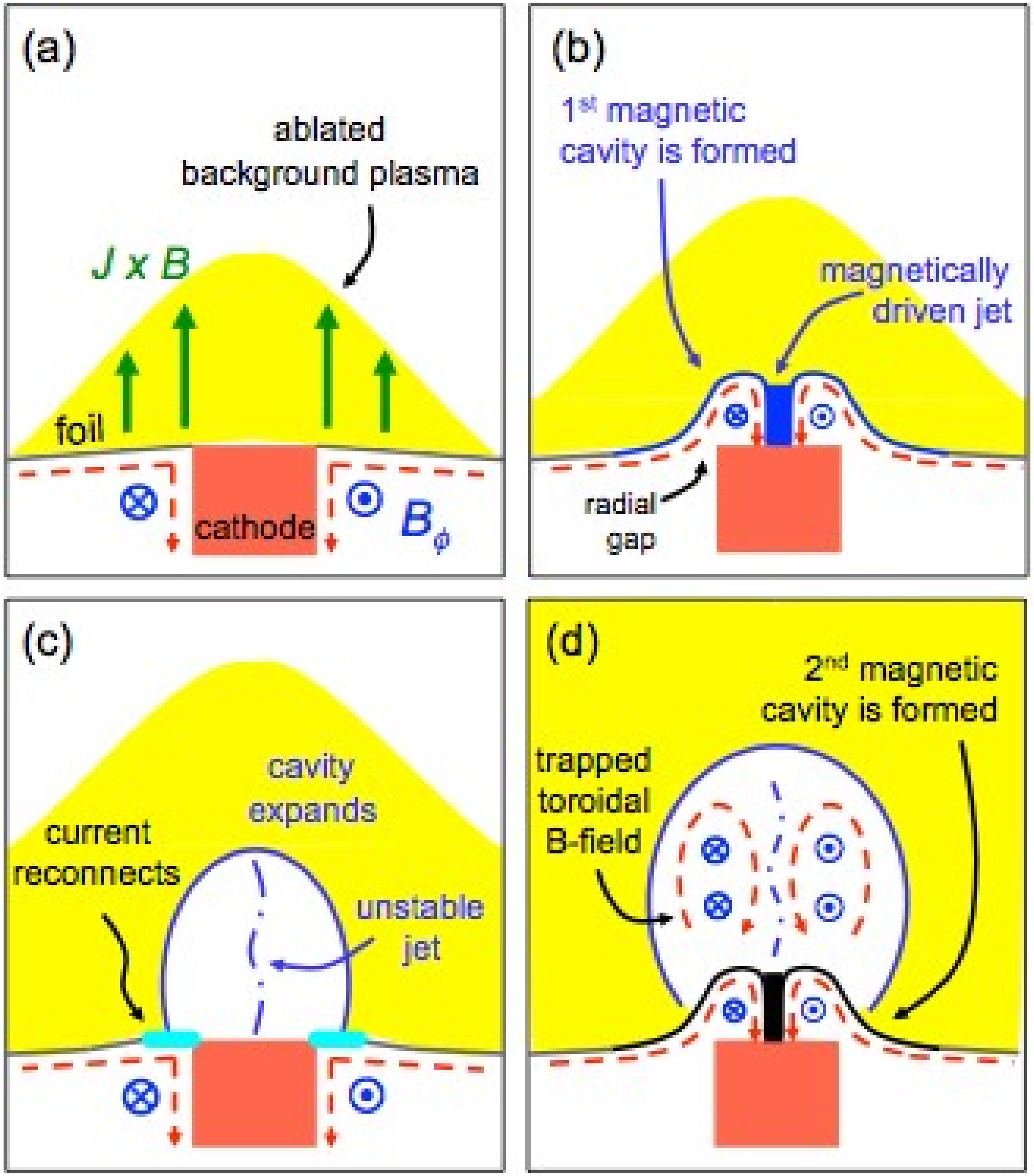

(a)
ablated
background plasma
J x B
foil
cathode
B_ϕ
(b)
1st magnetic
cavity is formed
magnetically
driven jet
radial
gap
(c)
cavity
expands
current
reconnects
unstable
jet
(d)
2nd magnetic
cavity is formed
trapped
toroidal
B-field

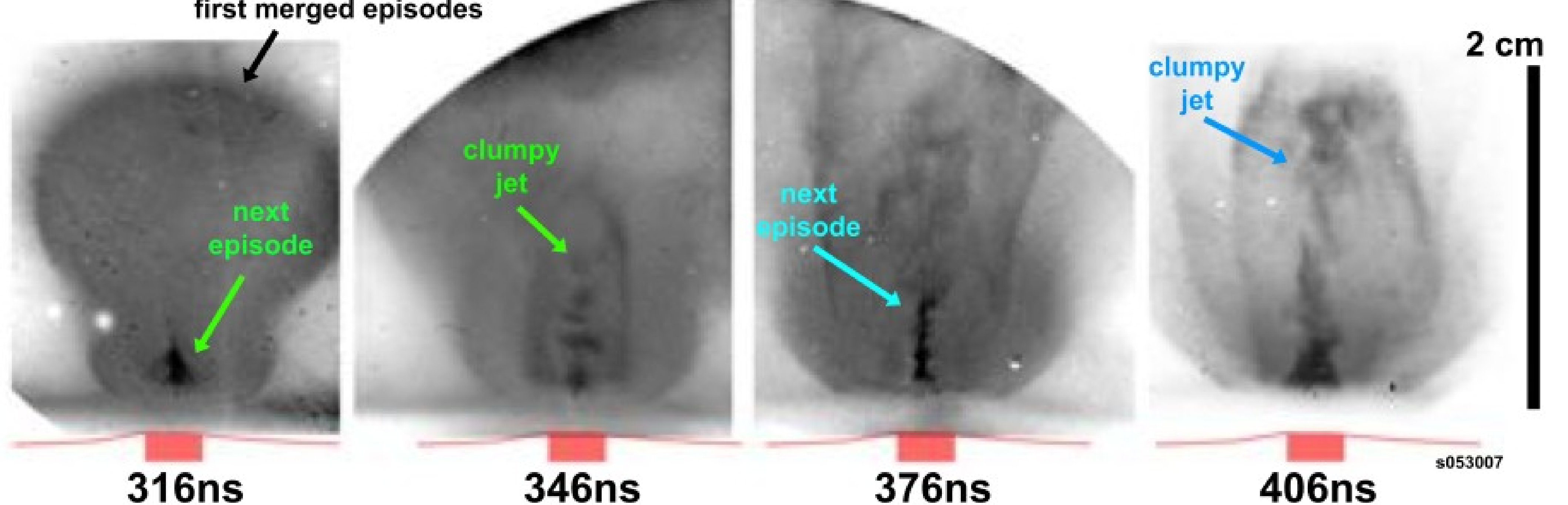

episodic

Suzuki-Vidal et al. 2011

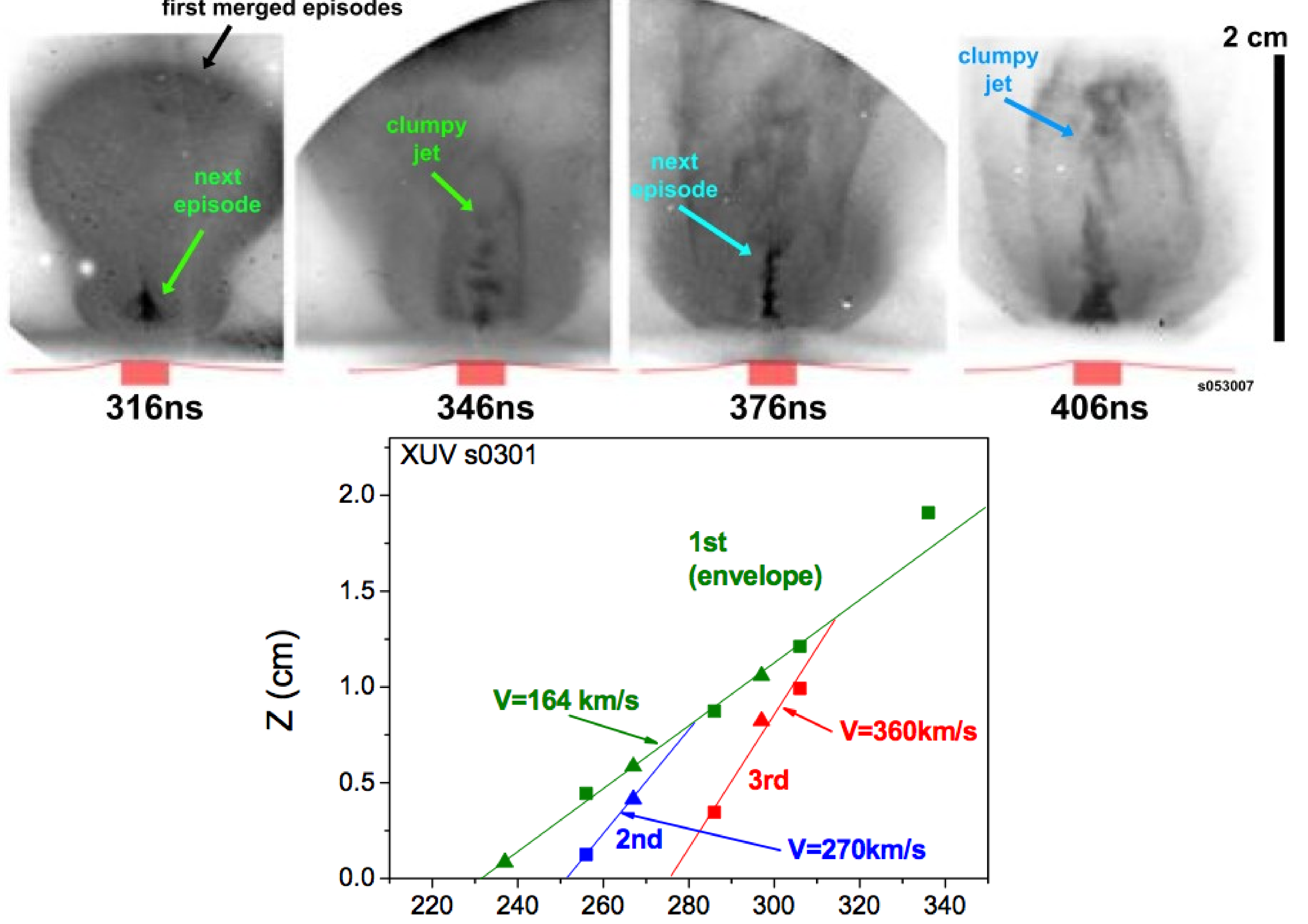

Suzuki-Vidal et al. 2011

We simulate stellar magnetic towers
(Huarte-Espinosa, Frank and Blackman 2011b, in prep)

THE ASTROPHYSICAL JOURNAL SUPPLEMENT SERIES, 182:519–542, 2009 June
doi:10.1088/0067-0049/182/2/519

code

SIMULATING MAGNETOHYDRODYNAMICAL FLOW WITH CONSTRAINED TRANSPORT AND ADAPTIVE MESH REFINEMENT: ALGORITHMS AND TESTS OF THE AstroBEAR CODE

ANDREW J. CUNNINGHAM[1], ADAM FRANK[1], PEGGY VARNIÈRE[1,2], SORIN MITRAN[3], AND THOMAS W. JONES[4]

- Solve hyperbolic PDE with elliptic constraints: **MHD**

- Source terms for energy loss/gain, **ionization dynamics**

- Operator splitting: **gravity, heat conduction** (*HYPRE*)

$$\frac{\partial}{\partial t}\begin{bmatrix} \rho \\ \rho v_x \\ \rho v_y \\ \rho v_z \\ \mathcal{E} \\ B_x \\ B_y \\ B_z \end{bmatrix} + \frac{\partial}{\partial x}\begin{bmatrix} \rho v_x \\ \rho v_x^2 + P + B^2/2 - B_x^2 \\ \rho v_y v_x \\ \rho v_z v_x \\ (\mathcal{E} + P + B^2/2)v_x - B_x(B \cdot v) \\ 0 \\ -E_z \\ E_y \end{bmatrix} +$$

$$\frac{\partial}{\partial y}\begin{bmatrix} \rho v_y \\ \rho v_x v_y \\ \rho v_y^2 + P + B^2/2 - B_y^2 \\ \rho v_z v_y \\ (\mathcal{E} + P + B^2/2)v_y - B_y(B \cdot v) \\ E_z \\ 0 \\ -E_z \end{bmatrix} + \frac{\partial}{\partial z}\begin{bmatrix} \rho v_z \\ \rho v_x v_z \\ \rho v_y v_z \\ \rho v_z^2 + P + B^2/2 - B_z^2 \\ (\mathcal{E} + P + B^2/2)v_y - B_z(B \cdot v) \\ -E_y \\ E_x \\ 0 \end{bmatrix} = S$$

$$\nabla \cdot B = 0.$$

AstroBEAR 2.0
Parallel AMR Performance

Rebuild load balance algorithm across AMR grid hierarchy (Carroll et al. 2011, in prep.)

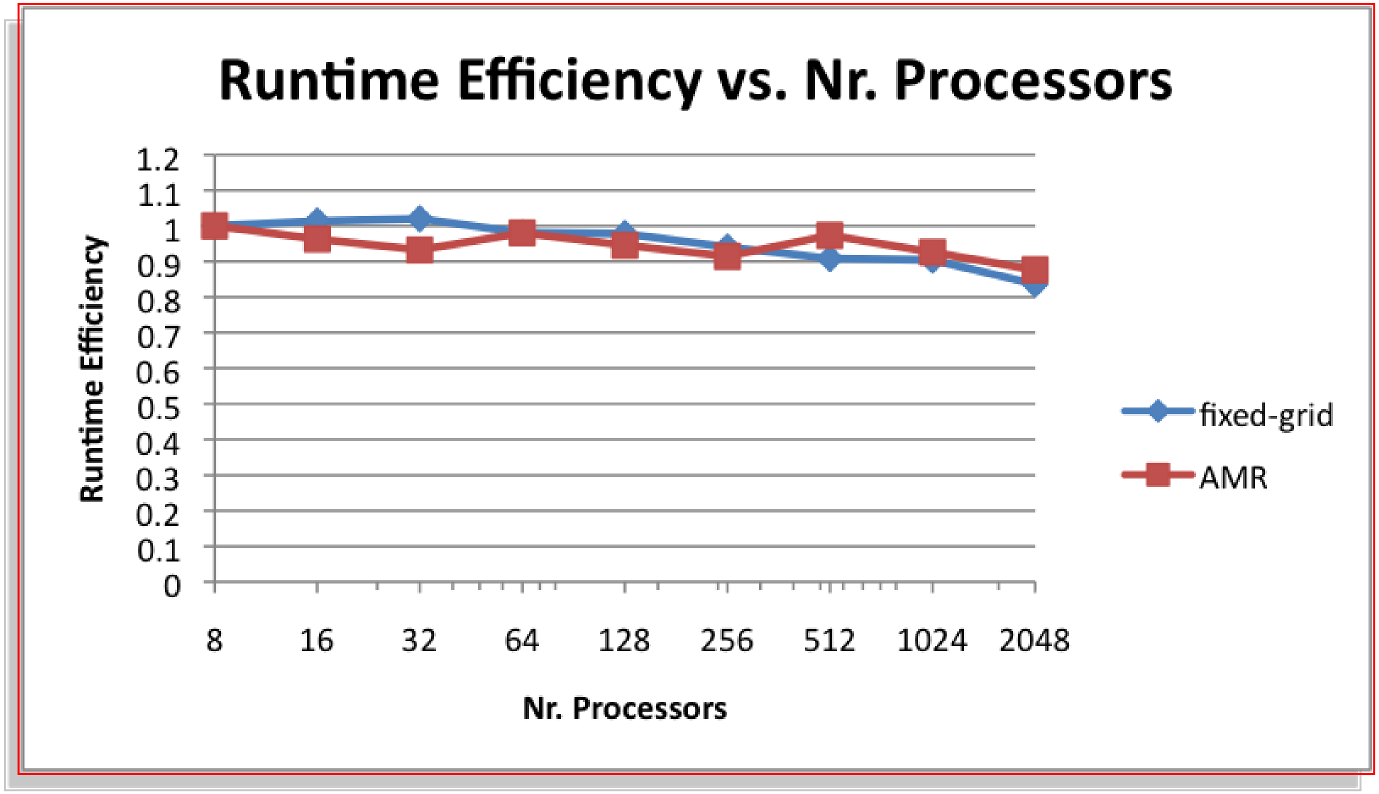

https://clover.pas.rochester.edu/trac/astrobear

Our simuations

In Huarte-Espinosa, Frank and Blackman (2011b, in prep.) we use AstroBEAR2.0 (Carroll et al. 2011, in prep.) to **solve the equations of radiative-MHD in 3D with AMR.**

1. Adiabatic PFD

2. Cooling PFD

3. Adiabatic and rotating PFD

4. Hydrodynamic jet with the same propagation speed and energy flux than the adiabatic run.

Initial conditions

Density = 100 cm^{-3}
Temperature = 10000 K
molecular gas, γ =5/3
V = 0 km s^{-1}.

Magnetic fields **only** within the central region

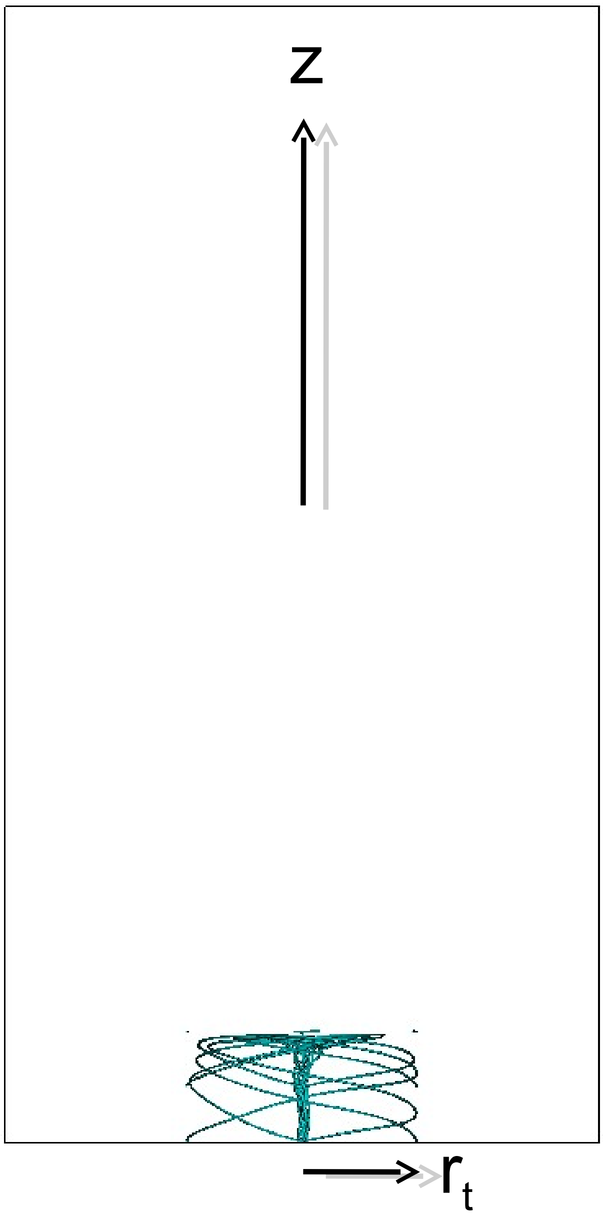

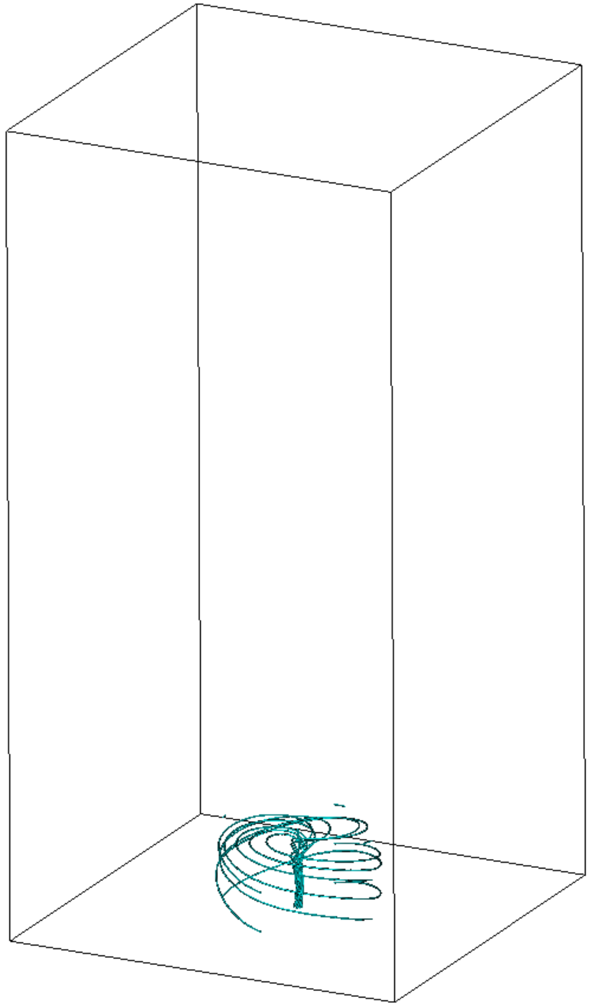

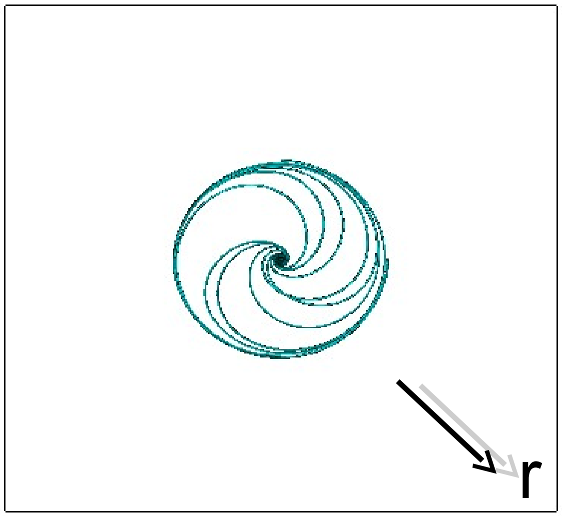

Continuous magnetic energy injection

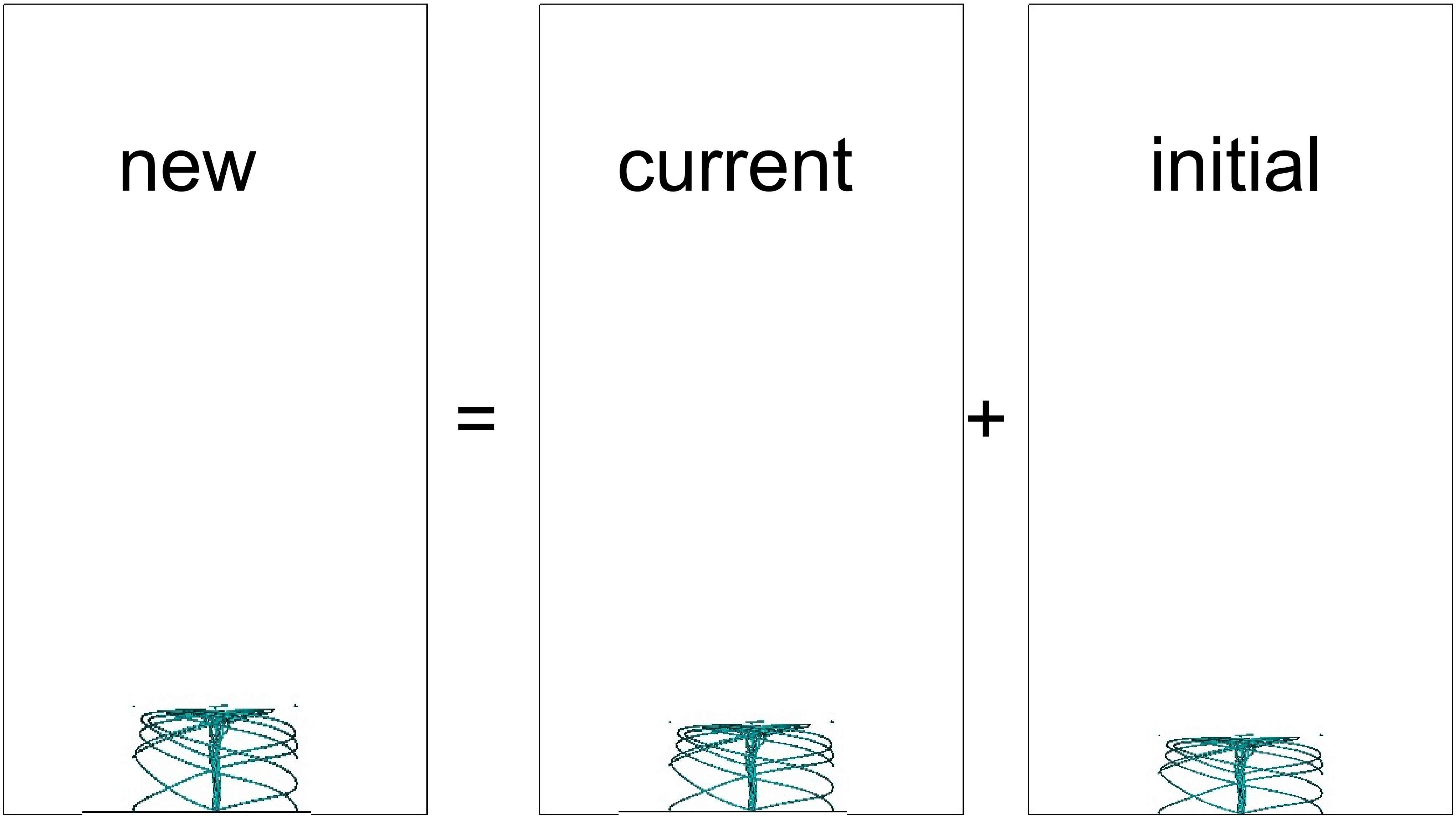

Adiabatic

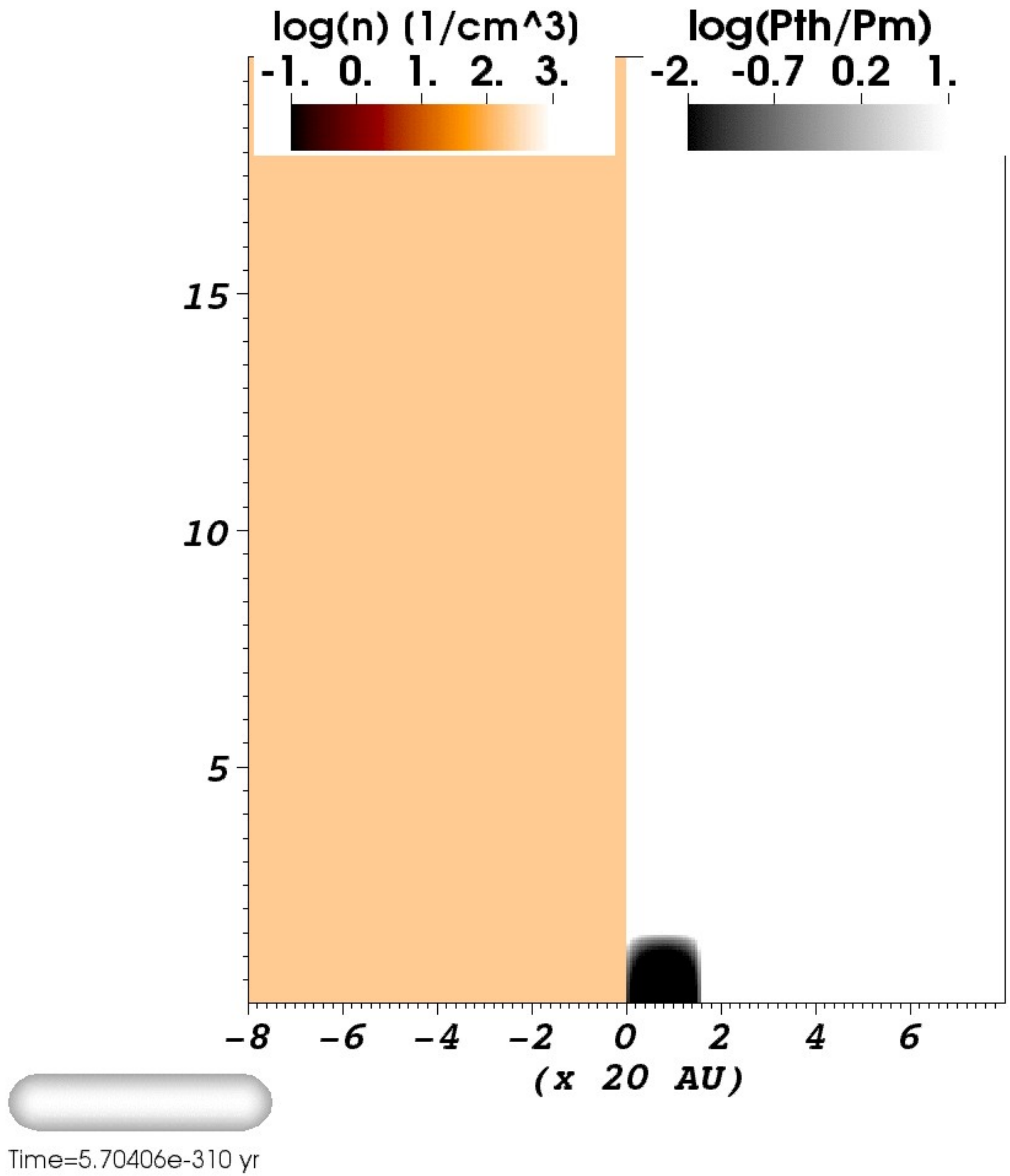

log(n) (1/cm^3)
-1. 0. 1. 2. 3.
log(Pth/Pm)
-2. -0.7 0.2 1.
15
10
5
−8 −6 −4 −2 0 2 4 6
(x 20 AU)
Time=5.70406e-310 yr

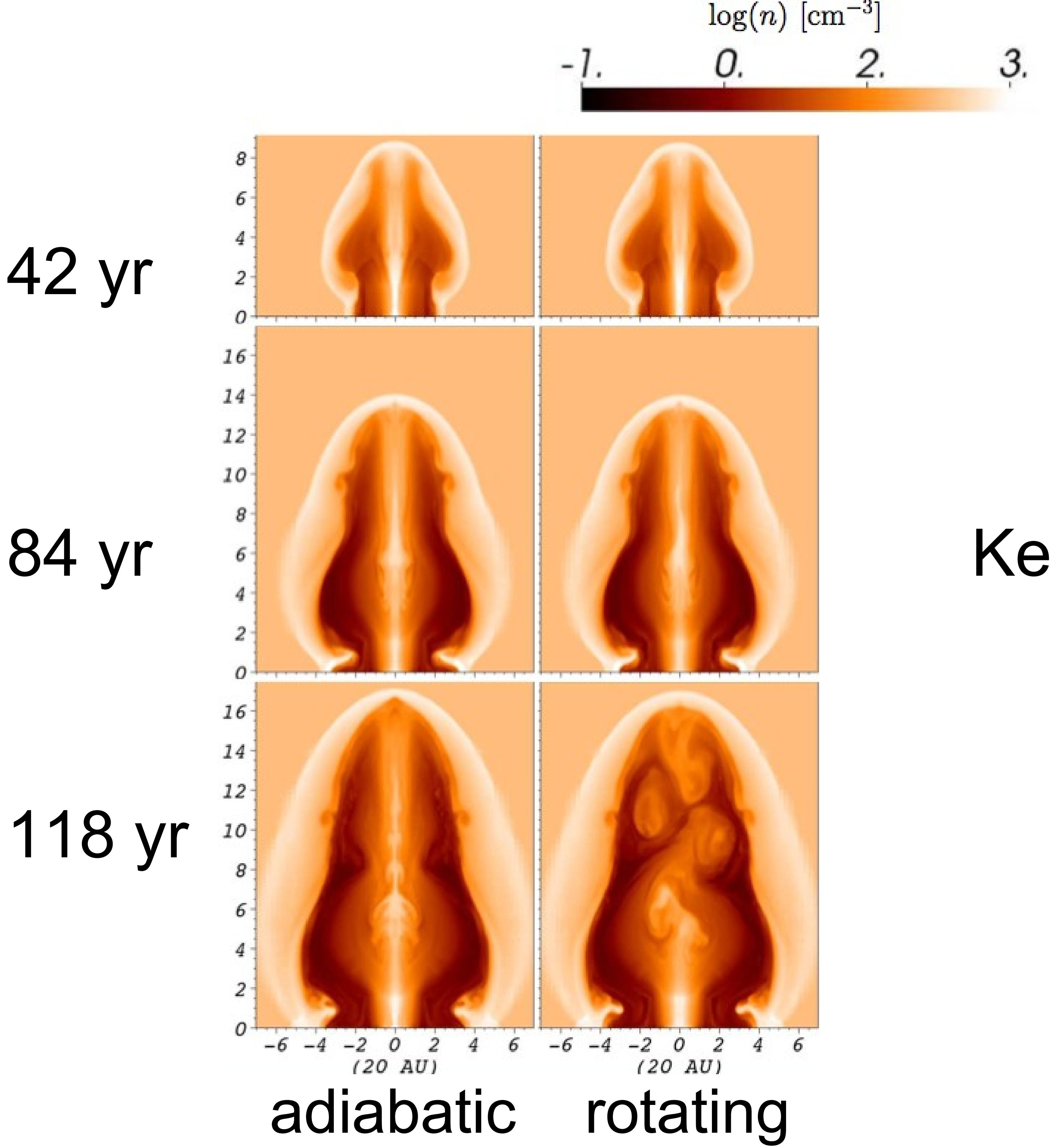

Keplerian

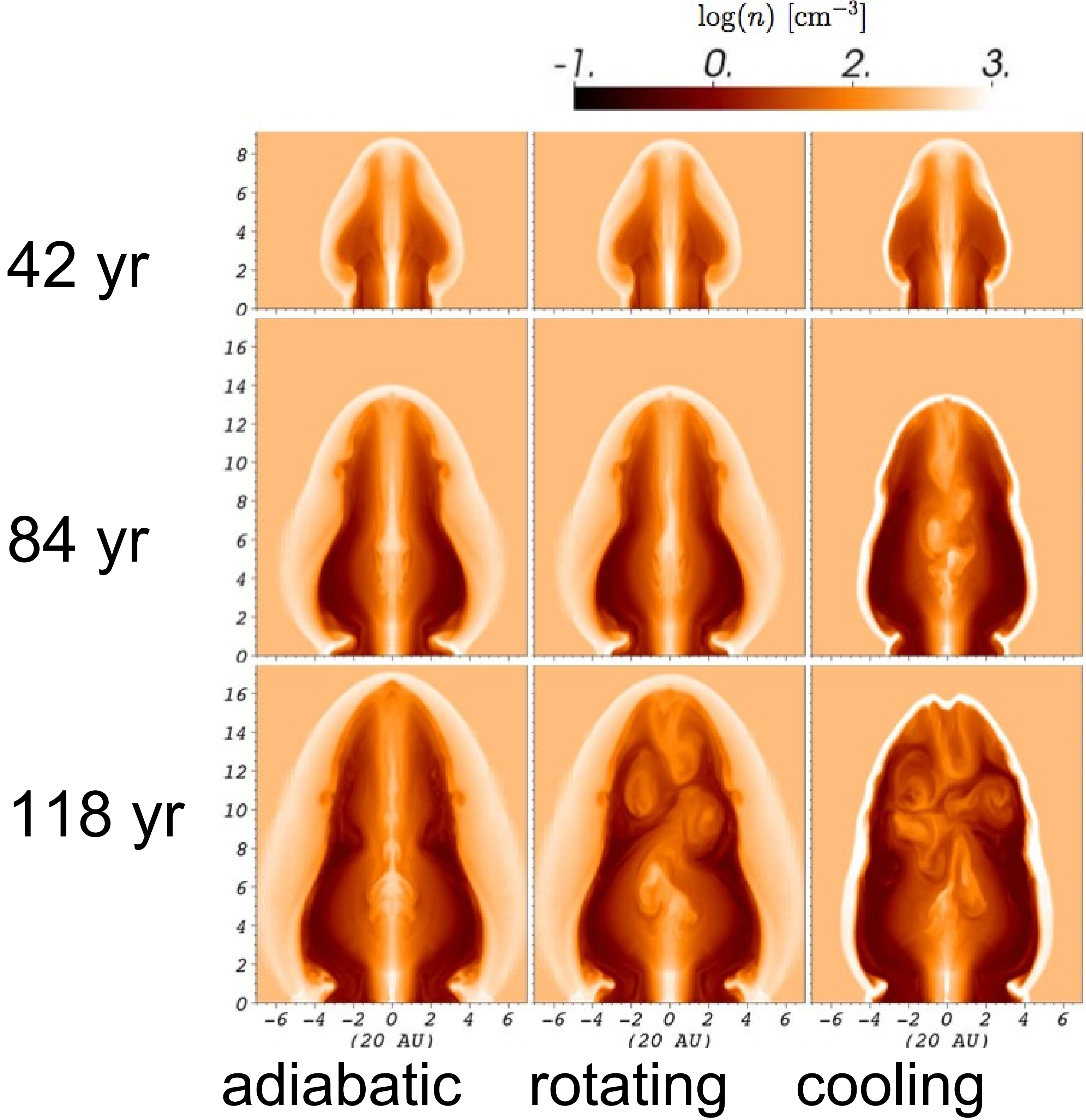

log(n) [cm^-3]
-1.
0.
2.
3.
42 yr
84 yr
118 yr
(20 AU)
adiabatic
rotating
cooling

Cooling

Dalgarno & Mccray (1972). Ionization of both H and He, the chemistry of H2 and optically thin cooling.

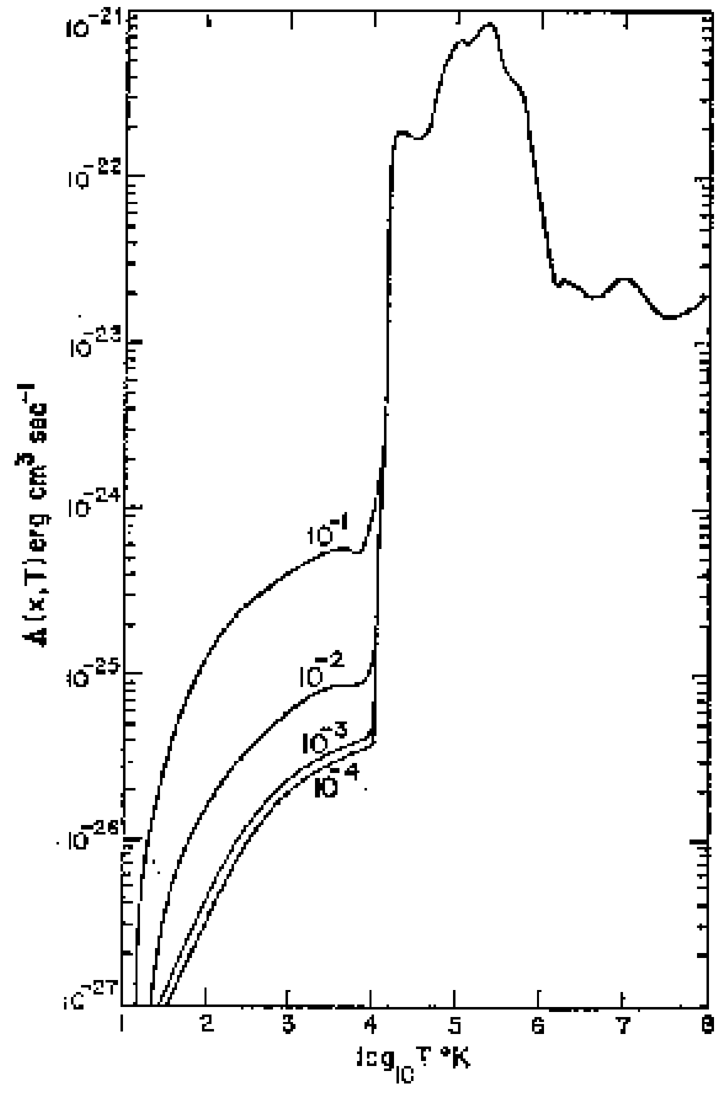

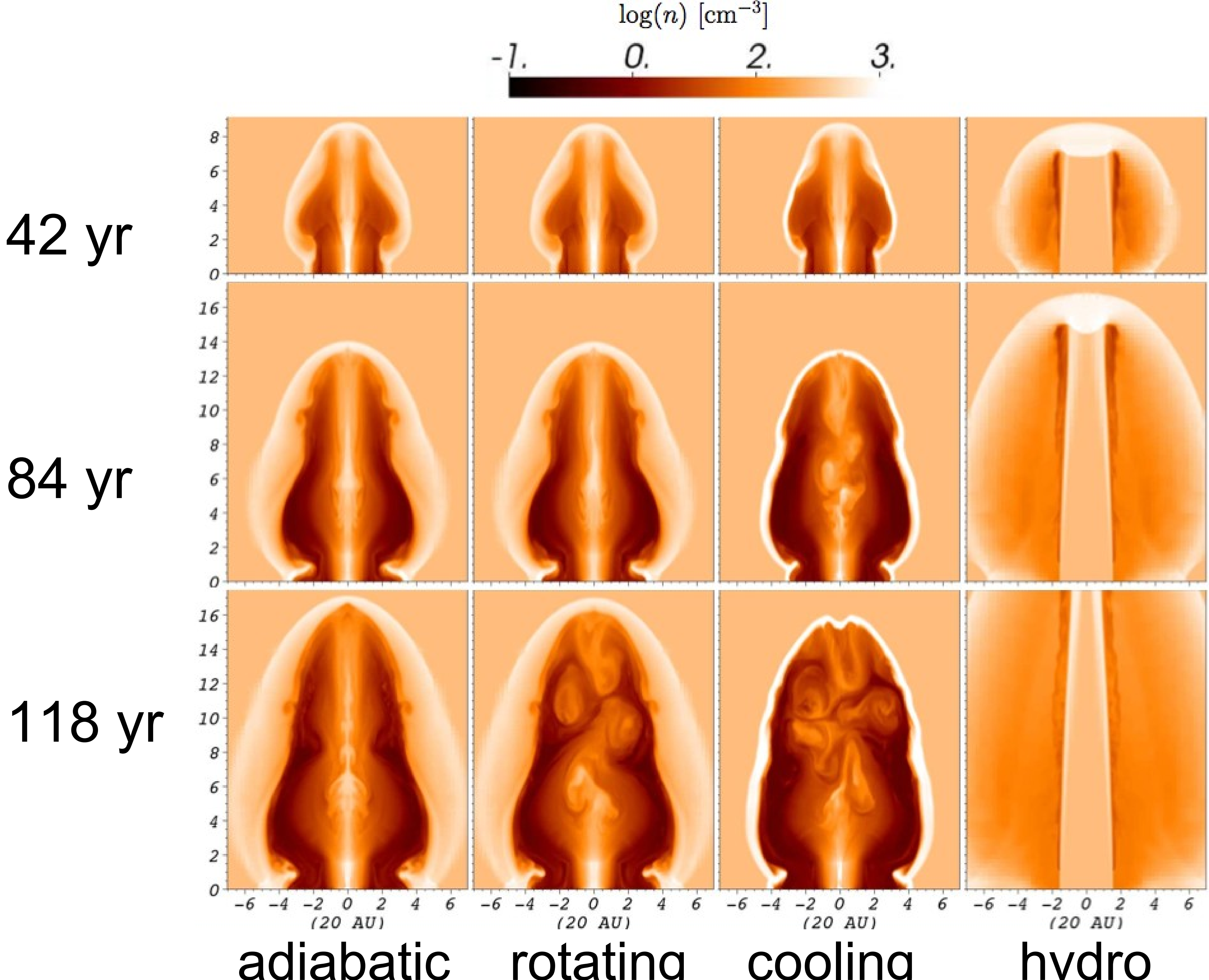

log(n) [cm^-3]
-1.
0.
2.
3.
42 yr
84 yr
118 yr
(20 AU)
adiabatic
rotating
cooling
hydro

Field line maps

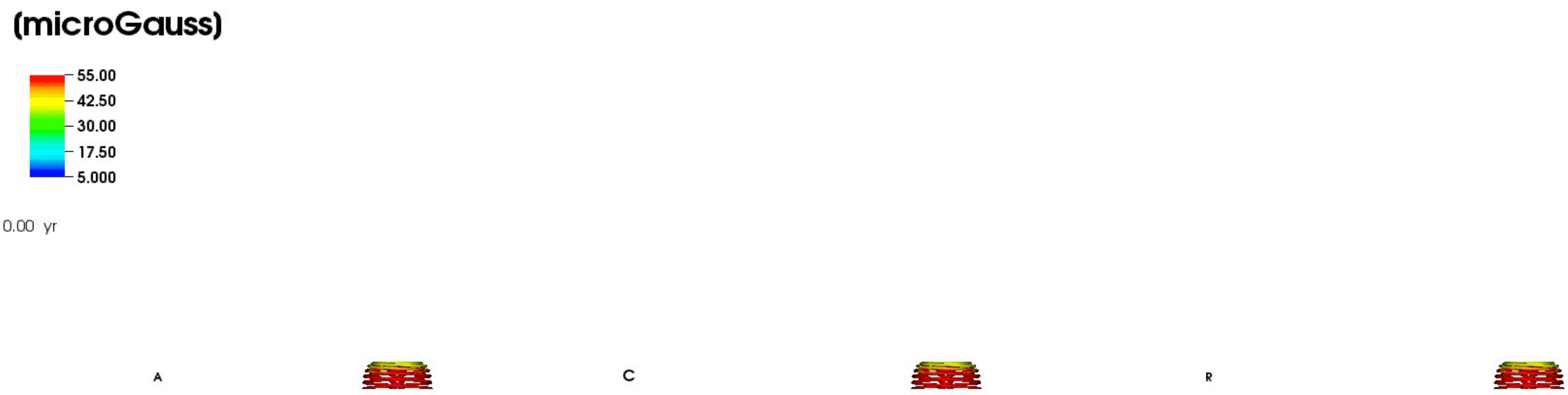

adiabatic **cooling** **rotating**

Only 2 central field lines

Field geometry

HH 81-81 (Carrasco-González et al. '10)

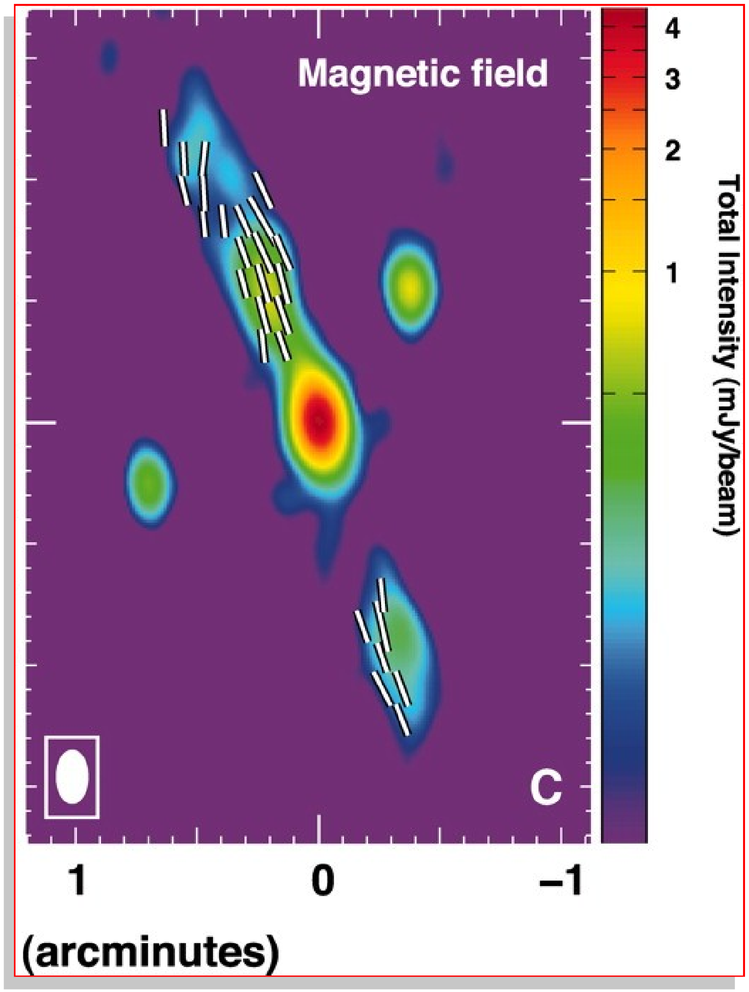

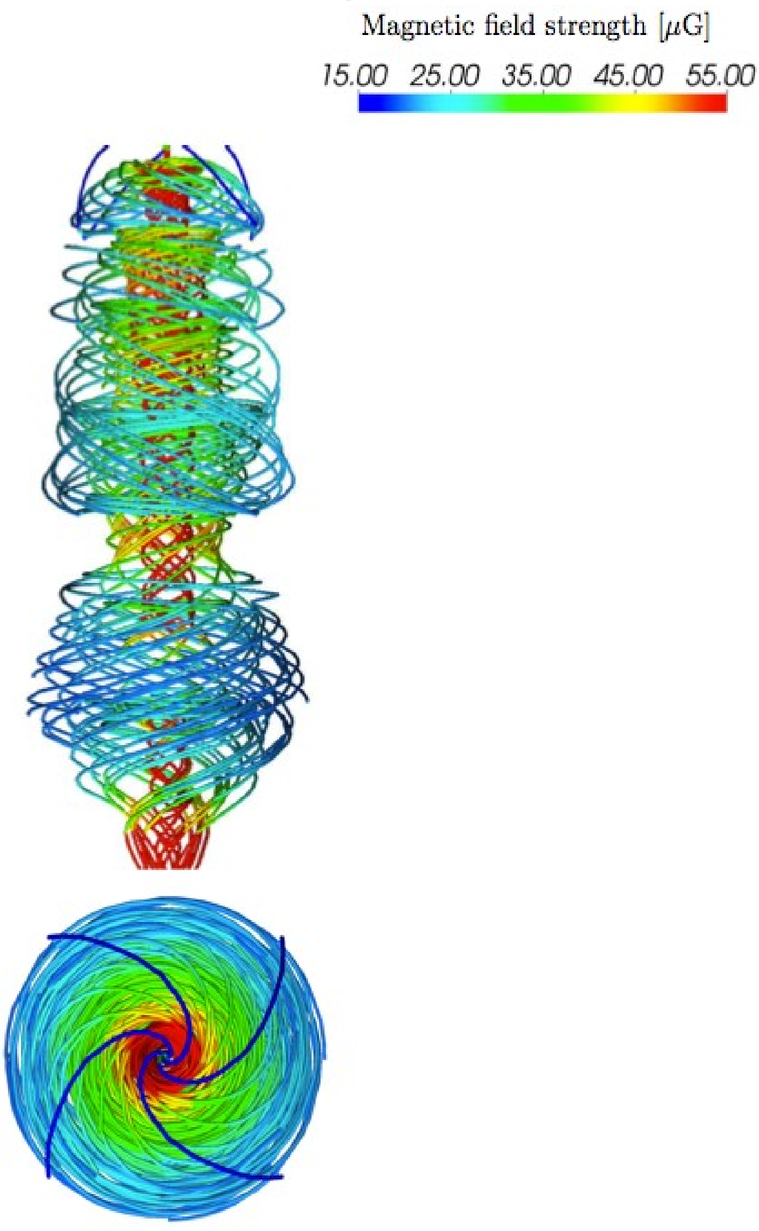

Adiabatic

consistent ☺

Perturbations

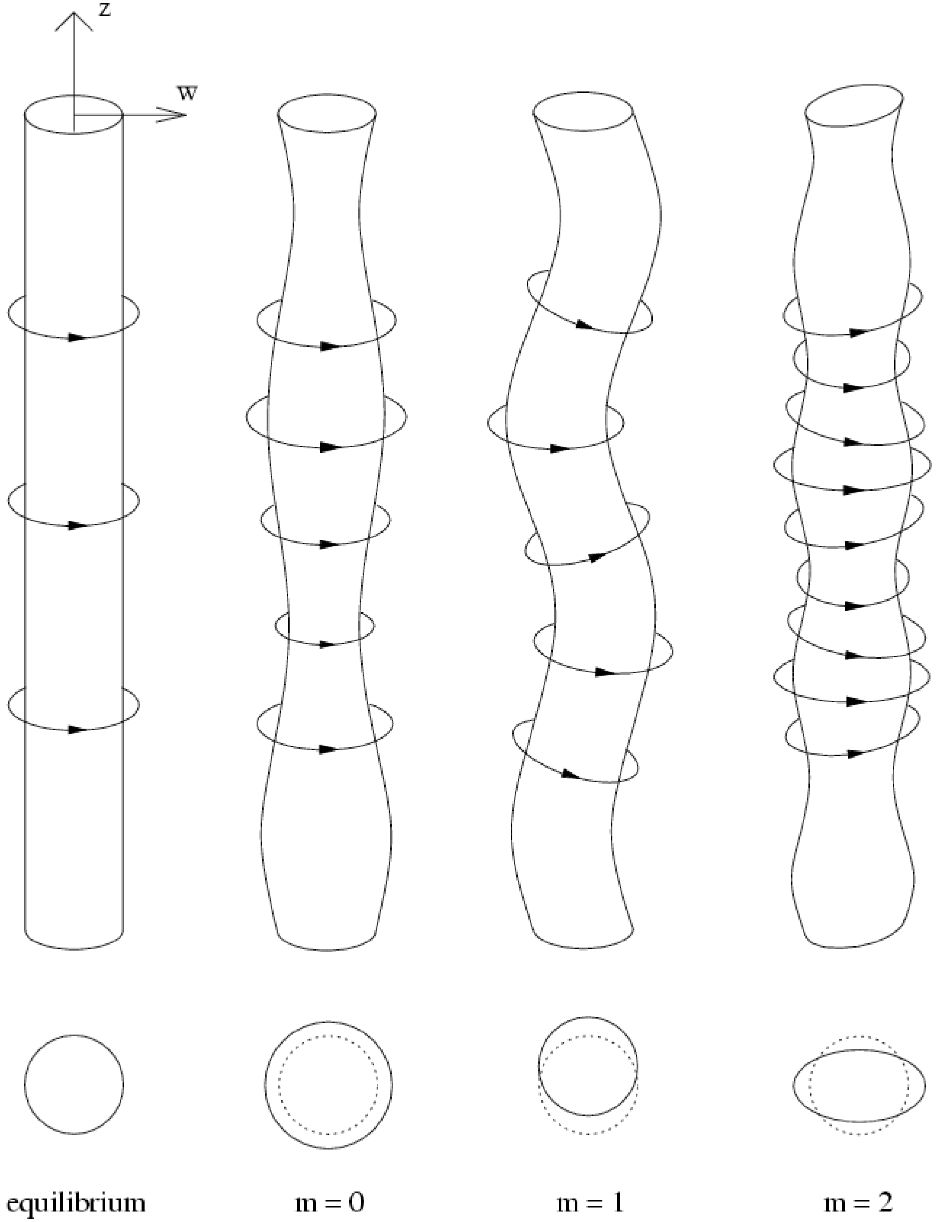

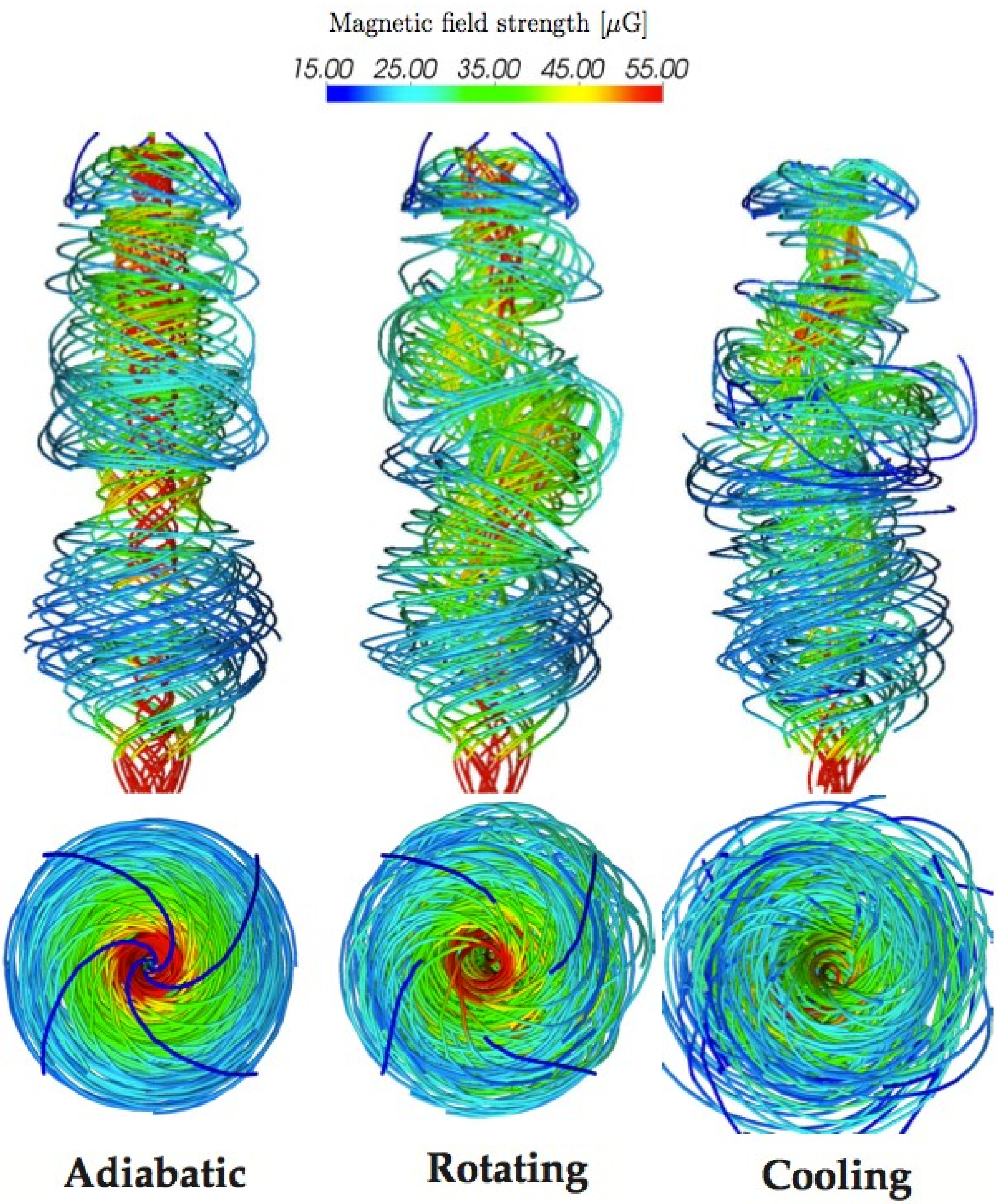

Instability:

$$\left|\frac{B_\phi}{B_z}\right| > |(\beta_z - 1)kr_{jet}|$$

where $\beta_z = 2\mu_0 P/B_z^2$.

Relative strength:

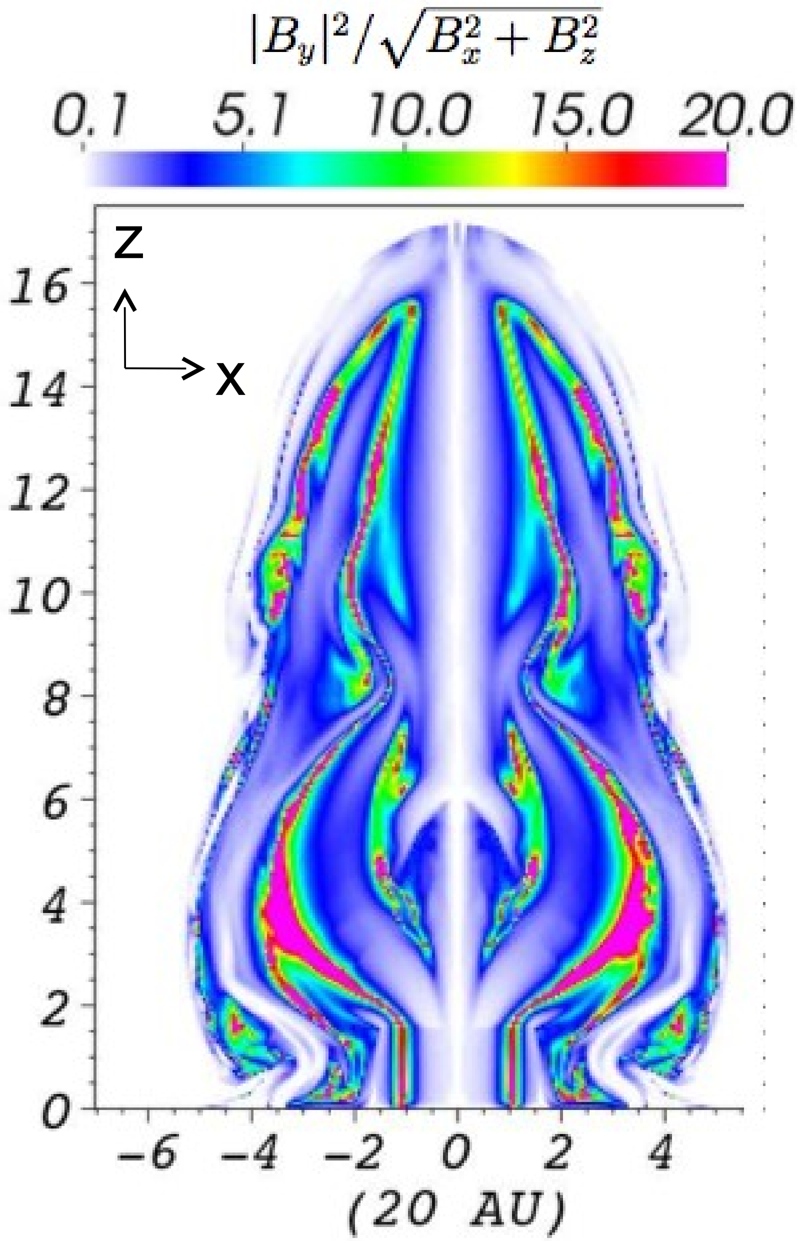

Jet velocities:

$$\left|\frac{B_\phi}{B_z}\right| > |(\beta_z - 1)kr_{jet}|$$

where $\beta_z = 2\mu_0 P/B_z^2$.

Alfvén speed highest inside tower

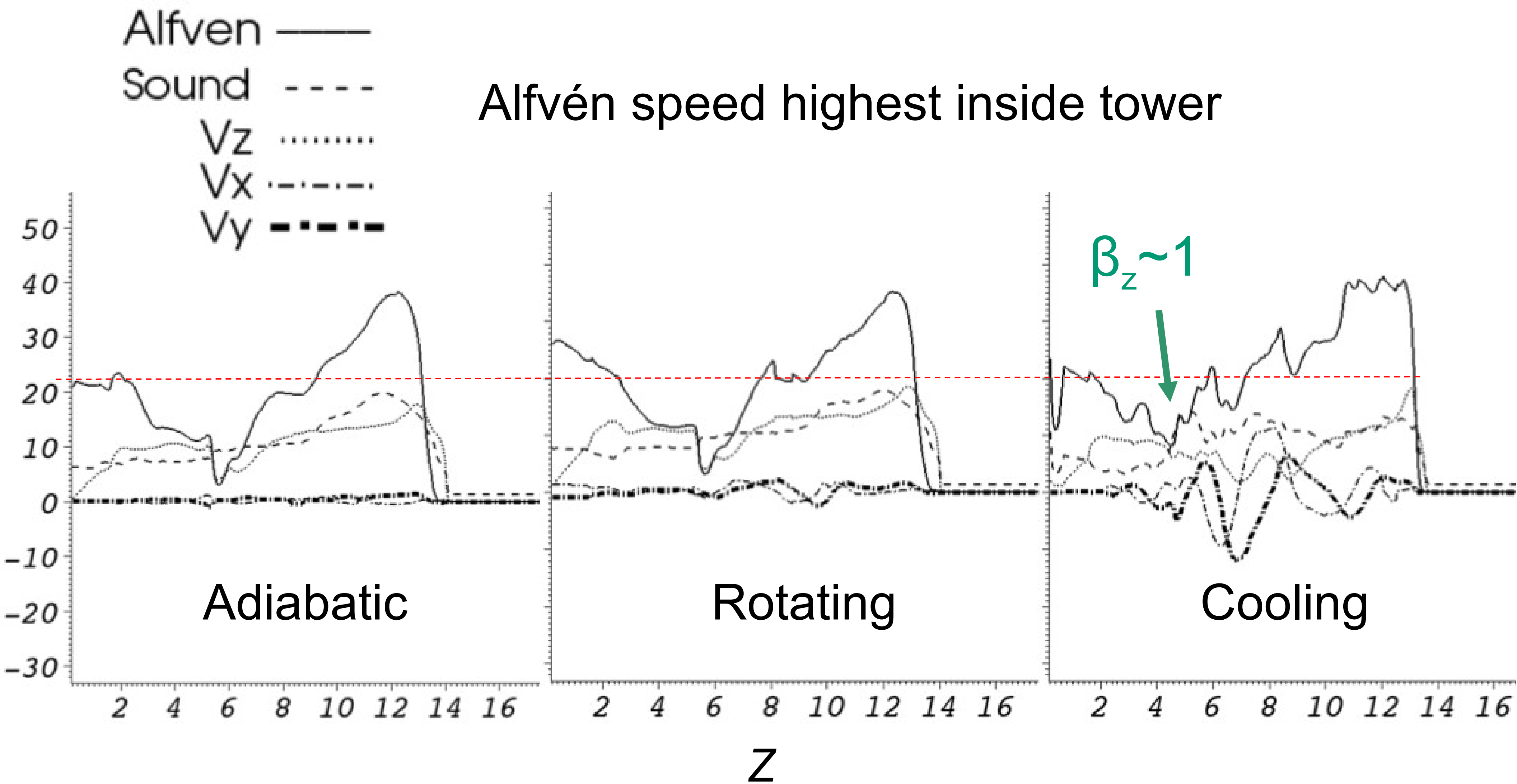

Current

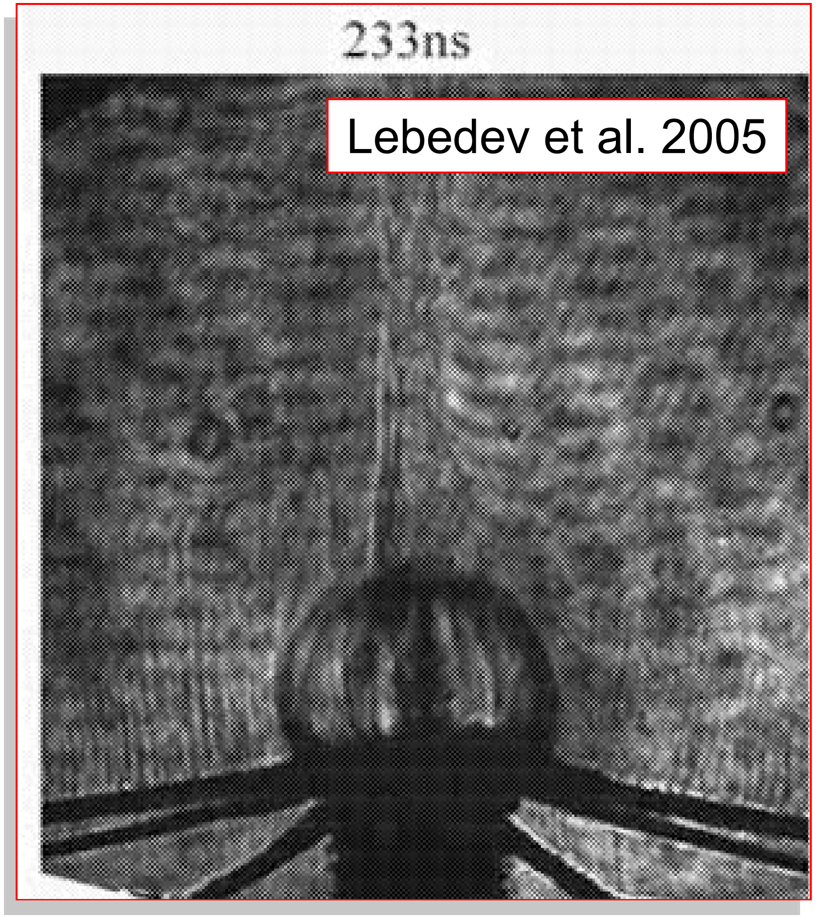

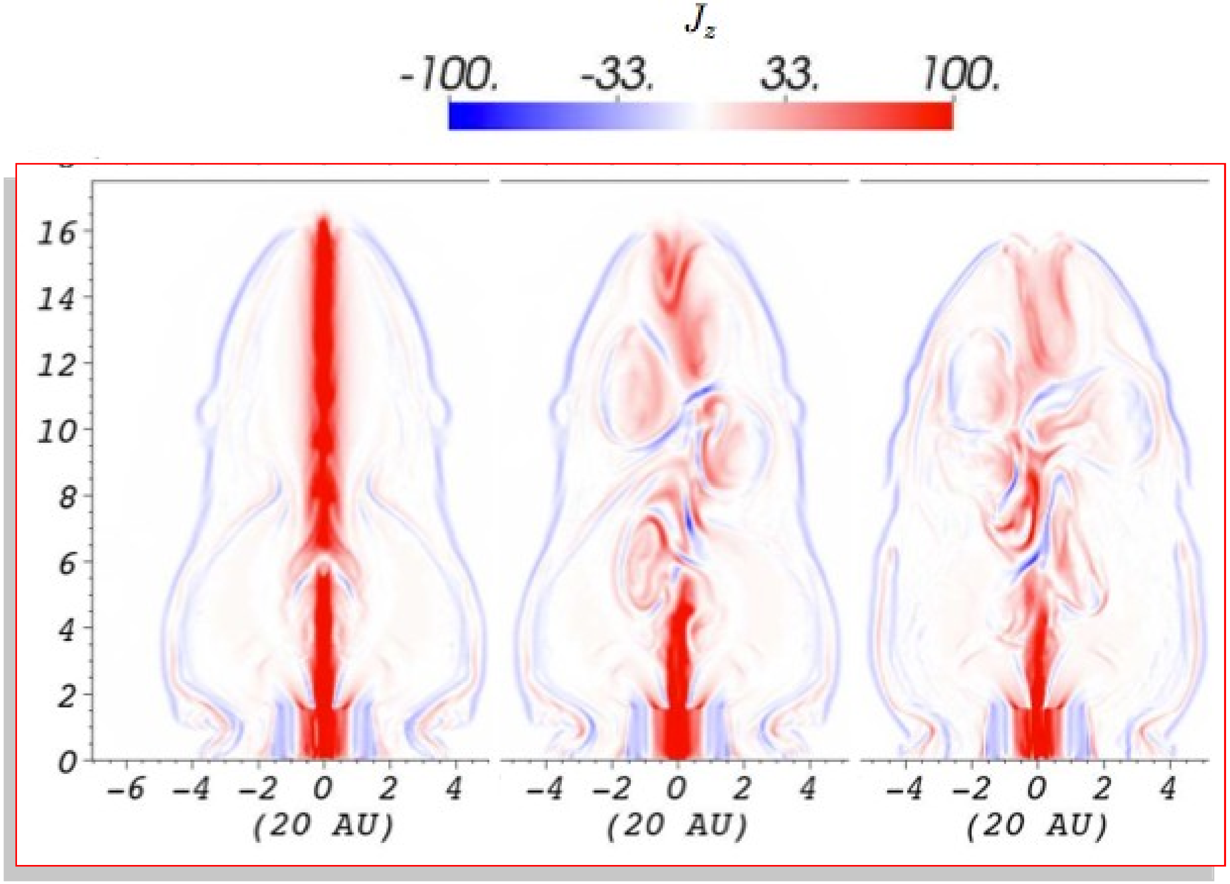

Adiabatic Rotating Cooling

consistent ☺

See ***poster*** for details

Modeling Poynting flux vs. kinetic-energy dominated jets

Huarte-Espinosa, Frank & Blackman

Modeling Poynting flux vs. kinetic-energy dominated jets

Martín Huarte-Espinosa†, Adam Frank and Eric Blackman.
Department of Physics and Astronomy, University of Rochester, Rochester NY, USA.
† martinhe@pas.rochester.edu

Introduction

Jets are observed in the vicinities of Protostellar Objects, Young Stellar Objects (YSOs), post-AGB stars, X-ray binaries and active galactic nuclei. Models suggest that jets are launched and collimated by accretion, rotation and magnetic mechanisms in their "central engine" (review [1]). The extent over which the magnetic energy of jets dominates the kinetic energy divides them into (i) magnetocentrifugal jets [2], in which magnetic fields only dominate out to the Alfvén radius, (ii) Poynting flux dominated jets [3,4] (PFD), in which magnetic fields dominate the jet structure. Recent laboratory experiments have produced magnetized jets [5].

Open questions: What is the relation between the main observable features (length, velocity, cocoon geometry, etc.) of PFD jets and their power (this is known for kinetic-energy dominated (magnetocentrifugal) jets)? What is the effect of cooling and rotation on PFD jets? The image below is from [8].

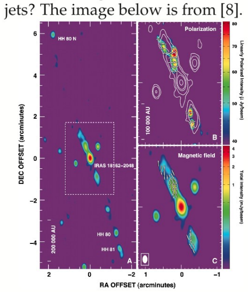

Model

We use the Adaptive Mesh Refinement (AMR) code *AstroBEAR2.0* [6] to solve the equations of radiative-MHD in 3D. The domain: $|x|, |y| \leq 160$ AU and $0 \leq z \leq 400$ AU, $64 \times 64 \times 80$ cells plus 2 AMR levels; resolution of 1.25 AU.

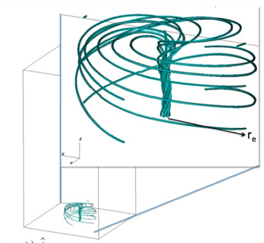

Initial conditions:
- Static molecular gas
- Ideal gas eqn. of state ($\gamma = 5/3$)
- $n = 100\,\mathrm{cm}^{-3}$; $T = 10000$ K
- $$\mathbf{A}(r,z) = \begin{cases} \frac{r}{4}(cos(2\,r)+1)(cos(2\,z)+1)\hat{\phi} + \\ \frac{\alpha}{8}(cos(2\,r)+1)(cos(2\,z)+1)\hat{k}, & \text{for } r,z < r_e; \\ 0, & \text{for } r,z \geq r_e, \end{cases}$$
- $r_e \sim 30$ AU; $\alpha = 40$ ($= 800$ AU); $\beta < 1$ for $r, z < r_e$.

Evolution: Continuous central injection of magnetic or kinetic energy.

Simulations:
- *Magnetic towers*: adiabatic; optically thin cooling [7]; Keplertian rotation
- *Hydrodynamical jet* with the same time average propagation speed and energy flux than the adiabatic magnetic tower.

Structure and evolution

Magnetic pressure pushes field lines and plasma up, forming magnetic cavities with low density. The adiabatic case is the most stable. Towers decelerate relative to the hydro jet; magnetic energy pressure produces axial but also radial expansion. Towers' jets (cores) are thin and unstable, whereas the hydro jet beam is thicker, smoother and stable.

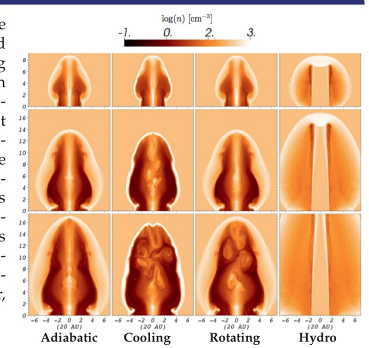

Time= {42, 84, 118} yr, from top to bottom.

Forces and current density

Magnetic pressure dominates over thermal. Towers' jets (cores) are confined by the magnetic hoop stress from surrounding field lines. The cavity is collimated by external thermal pressure.

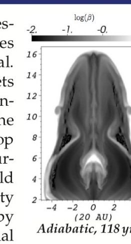

Adiabatic, 118 yr

Towers' jets carry a high axial current density. There is a current-free region about the jets. The main return current goes along the cavity's outer contact discontinuity.

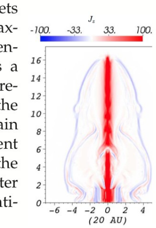

Adiabatic, 118 yr

Field geometry and stability

The jets' field lines are parallel to $r = 0$ and surrounded by toroidal lines (red). There is another exterior helical component of lines. The injected magnetic energy keeps a non-force-free configuration at base; "new" lines push "old" ones upwards. Independently, cooling and rotation amplify current-driven perturbations. We see pinch (m=0) and kink ($m = 1$) modes. The Figure's time is 118 yr.

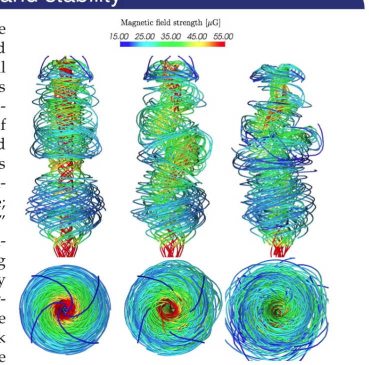

Jet velocity field, shocks and wave fronts

v_x, v_y, $v_z (= v_{jet})$, the sound and the Alfvén speed of the towers at $r = 0$. Early, jets are sub-Alfvénic and trans-sonic. Fast-forward MHD (FF) and hydrodynamic shocks are formed ahead of the jets' head. FF shocks steepen in time. Hydrodynamic shocks are quickly affected by cooling. The adiabatic and rotating cases show high beta regions between the reverse and the forward slow-modes of compressive MHD waves. Late, the cooling and rotating jets show fast, azimuthal, sub-Alfvénic velocities in their central beam part.

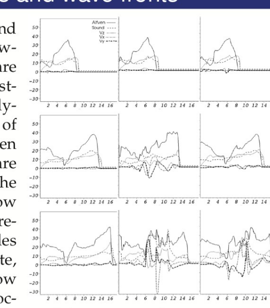

Time= {42, 84, 118} yr, from top to bottom.

Conclusions

- PFD jet beams are lighter, slower and less stable than kinetic-energy dominated ones. We predict characteristic emission distributions for each of these.
- Current-driven perturbations in PFD jets are amplified by both cooling, firstly, and base rotation, secondly: shocks and thermal pressure support are weakened by cooling. Total pressure balance at the jets' base is affected by rotation.
- Our models agree well with [3,4,5,8].

References

[1] Pudritz, R. E., et al., 2007, Protostars and Planets V, 277; **[2]** Blandford, R. D., & Payne, D. G. 1982, MNRAS, 199, 883; **[3]** Lynden-Bell, D. 1996, MNRAS, 279, 389; **[4]** Nakamura, M., & Meier, D. L. 2004, ApJ, 617, 123; **[5]** Lebedev, S. V., et al. 2005, MNRAS, 361, 97; **[6]** Cunningham A. J. et al., 2009, ApJS, 182, 519 (https://clover.pas.rochester.edu/trac/astrobear/wiki/WikiStart); **[7]** Dalgarno A., McCray R. A. 1972, ARA&A, 10, 375; **[8]** Carrasco-González, C. et al., 2010, Science, 330, 1209

Acknowledgements

Financial support for this project was provided by the Space Telescope Science Institute grants HST-AR-11251.01-A and HST-AR-12128.01-A; by the National Science Foundation under award AST-0807363; by the Department of Energy under award DE-SC0001063; and by Cornell University grant 41843-7012.

Summary

About the experiments of Lebedev, Suzuki-Vidal et al.:

-PFD jets can be produced in the lab!, and help to understand the physics of astrophysical jets

-Lab jets collimated by hoop stress; outer magnetic cavities collimated by external pressure

-Lab jets show physical characteristics consistent with observation of galactic jets

-B_z affects the axial compression/expansion and the jet stability

-Jets adopt wiggled structures due to current-driven instabilities

-Thin conduction foils produce episodic jets and nested magnetic bubbles. New structures are faster than old ones.
e.g. Episodic jets in the FRII B0925+420 (Brocksopp at al. ‘07)

Summary

About our simulations:

-Good agreement with Lynden-Bell ’96; Nakamura & Maier ’04; Li et al. ’06; Lebedev et al. ‘05, ‘10; Ciardi et al. ’07; Suzuki-Vidal et al. ’10,

-PFD jet beams are lighter, slower and less stable than kinetic-energy dominated ones,

-We predict characteristic emission distributions for each of these,

-Current-driven perturbations in PFD jets are amplified by both cooling, firstly, and base rotation, secondly,

-Shocks and thermal pressure support are weakened by cooling,

-Total pressure balance at the jets’ base is affected by rotation.

Summary

About our simulations:

-Good agr... Maier ’04; Li et al. ’06 ... uzuki-Vidal et al. ’10,

-PFD jet beams are lighter, slower and less stable than kinetic-energy dominated ones,

-We predict characteristic emission distributions for each of ...

... cooling, firstly, and base rotation, secondly,

-Shocks and thermal pressure support are weakened by cooling,

-Total pressure balance at the jets’ base is affected by rotation.

Thanks!

Find this talk at: http://www.pas.rochester.edu/~martinhe/talks.html